FUNDAMENTALS, PREPARATION, AND CHARACTERIZATION OF SUPERHYDROPHOBIC WOOD FIBER PRODUCTS

A Thesis
Presented to
The Academic Faculty

by

Hongta Yang

In Partial Fulfillment
of the Requirements for the Degree
of Paper Science and Engineering in the
School of Chemical and Biomolecular Engineering

Georgia Institute of Technology
August, 2008

FUNDAMENTALS, PREPARATION, AND CHARACTERIZATION OF SUPERHYDROPHOBIC WOOD FIBER PRODUCTS

Approved by:

Dr. Yulin Deng, Advisor
School of Chemical and Biomolecular Engineering
Georgia Institute of Technology

Dr. Zhong Lin Wang
School of Materials Science and Engineering
Georgia Institute of Technology

Dr. Sujit Banerjee
School of Chemical and Biomolecular Engineering
Georgia Institute of Technology

Dr. Jeffery S. Hsieh
School of Chemical and Biomolecular Engineering
Georgia Institute of Technology

Date Approved: April 30, 2008

To my beloved family

ACKNOWLEDGEMENTS

I would like to express my deepest appreciation to Dr. Yulin Deng, who served as my thesis supervisor over the past two years, showing me different ways to approach and resolve the challenging research problems, and continuously giving me tolerance, encouragement, and advice in my research. With his broad knowledge, diligent working attitude, and optimistic and kind spirit in daily life, Dr. Yulin Deng acted not only as an academic mentor, but also as a good friend who impacted me in my future career. My special thanks go to Dr. Sujit Banerjee, Dr. Jeffery S. Hsieh, and Dr. Zhong Lin Wang for actively participating in my committee. I am grateful to the Institute of Paper Science and Technology for financial support of this research.

My appreciation to Dr. Qunhui Sun, who guided me into the world of nanotechnology, is beyond my expression. My great thanks are given to Dr. Yulin Zhao, for his valuable discussions in the papermaking filed; Ms. Yolande Berta, for her assistance and training in SEM; Dr. Jeng-Yue Wu, for providing tensile tester; Ms. Chunxu Dong, for her assistance with the bacteria resistance test; and all those people who kindly gave me assistance in my research work. It would have been impossible to complete this work without their efforts. Finally, I am indebted to my fellow graduate students, Mrs. Ying Wang, Mr. Zhengzhi Zhou, Mr. Jihoon Lee, Mr. Delong Song, and Dr. Kimberly Nelson, who always helped me in the lab.

TABLE OF CONTENTS

LIST OF FIGURES

SUMMARY

Wood fiber materials are hydrophilic which resulting in absorbing moisture and water easily. The solution for solving the problem is to increase the wood fiber hydrophobicity by modifying the wood fiber surface. The common surface treatments to increase the wood fiber hydrophobicity are sizing treatments or surface barrier coatings. Although paper sizing can increase the hydrophobicity of paper products, the water proof efficiency is not high enough for package applications. Barrier coating is one of the most important approaches for manufacturing high water resistance paper containers. However, the thick coating layer results in high coating cost and poor paper recyclability.

Superhydrophobic surfaces indicate the surfaces with water contact angle larger than 150^{o}. Compared with regular hydrophobic surfaces, superhydrophobic surfaces are with much higher anti-wetting property and better self-cleaning property. Superhydrophobic surfaces are usually prepared by combining an appropriate surface roughness with a hydrophobic material, since the hydrophobicity of a surface is determined by its chemical composition and topography.

In this study, a superhydrophobic paper was developed by layer-by-layer deposition of cationic polymer, poly(diallyldimethylammonium chloride) (poly-DADMAC) and negative charged silica particles followed with a fluorination treatment by chemical vapor deposition of 1H, 1H, 2H, 2H-perfluorooctyltriethoxysilane (POTS). The prepared superhydrophobic paper products have the following characteristics:

1. Excellent anti-wetting property.
2. High moisture resistance.

3. High water resistance.

4. Anti-biological contamination.

CHAPTER 1

INTRODUCTION

Wood fibers are typical hydrophilic natural materials. With biodegradability, recyclability, and low cost, wood fibers have been widely used as package materials. The problem of using wood fiber material in packaging is its hydrophilicity resulting in high water and moisture absorption. The solution to solve the problem is to increase the wood fiber hydrophobicity. Hydrophobic substances are difficult to wet. The more hydrophobic a substance is, the more spherical the water bead and the higher the water contact angle. Once the hydrophobicity of wood fiber materials is increased, the anti-wetting property can be improved. Therefore, the hydrophobic wood fiber materials can be used to pack meat, fish, fruit, milk, and drinks fresh; the water-repellent wood fiber packages can also prevent the medicines from wetting; and the decomposable wood fiber products satisfy the green issue of the environment. The usual surface treatments to increase the wood fiber hydrophobicity are sizing treatments or barrier coatings.

1.1 The Use of Sizing Treatment on Paper/Linerboard Surface

The purpose of sizing treatment is to enable paper products to resist penetration by fluids and increase the hydrophobicity of surface. The treatment also provides better surface characteristics and improves certain physical properties of the paper sheet, such as surface strength and internal bond. Two basic methods of sizing are available to the papermaking: internal sizing and surface sizing. These are used either as sole treatments or in combination. Internal sizing utilizes rosin or other chemicals to reduce the rate of water penetration by reducing the surface energy, and thus the water contact angle.

Surface sizing typically utilized starch particles to fill in the surface voids in the sheets, reducing pore radius and therefore the rate of liquid penetration.

1.1.1 Internal Sizing Treatment on Paper/Linerboard Surface

Internal sizing can be achieved by using wet-end additives. The action of a wet-end sizing agent is to provide the fiber surfaces with a hydrophobic coating that discourages aqueous liquids from moving extensively. The traditional wet-end sizing agent is a modified rosin, most often in a saponified form to make it water soluble. Rosin size is usually shipped to the paper mill as a high-solids thick paste and is diluted through an emulsifier for metering into the stock. Natural rosin is the amber-colored resin obtained from southern pines. Formerly, it is tapped from growing trees or extracted from stumps. Now, more commonly, it is processed from tall oil. Rosin is an amphipathic material, meaning that it has both hydrophilic and hydrophobic parts. To provide good sizing, it is essential that the hydrophobic parts are oriented outward. In practice, the rosin is precipitated onto the fibers by the action of alum as an oriented monolayer of aluminum resinate molecules.

Rosins, along with wax emulsions, are sometimes categorized as non-reactive sizes. Their retention is dependent primarily on precipitate particle size and electrostatic attraction to cellulose. Also, they depend on the drying process to promote flow and coverage of the fiber surface. But, they do not react chemically with fibers.

Corresponding to the movement from traditional acidic papermaking toward a neutral or alkaline wet end, there is a trend toward greater use of synthetic sizing agents which react chemically with cellulose hydroxyl groups to form stable ester linkage. These chemicals were introduced to paper industry in the 1950s and provided the first

opportunity to manufacture sized paper in an alum-free environment. Alkyl ketene dimer was the first commercially available reactive size and is still the most widely used. Acrylic stearic anhydride sizes (derived from fatty acids) and alkenyl succinic anhydride (derived from petroleum) are more reactive and have more selective applications.

1.1.2 Surface Sizing Treatment on Paper/Linerboard Surface

Surface sizing is most commonly applied on machine at a station between dryer sections, which is referred to as the size press. For board grades, sizing solutions may be applied at the machine calendar stack. The most common material used in surface sizing solution is starch, either cooked or in a modified form. Starch is a carbohydrate synthesized in corn, tapioca, potato, and other plants by polymerization of dextrose units. The polymer exists in two forms: a linear structure of about 500 units and a branched structure of several thousand units. When an aqueous suspension is heated, the water is able to penetrate the granules and causes them to swell, producing a gelatinized solution. Wax emulsions or special resins are often added to the starch solution.

Sizing solution is commonly applied within a two roll nip; hence the term, size press. The traditional size press configurations are categorized as vertical, horizontal, or inclined. In each case, the objective is to flood the entering nip with sizing solution; the paper absorbs some of the solution and the balance is removed in the nip. The overflow solution is collected in a pan below the press and recirculated back to the nip. The retention time of the sheet in the pond and nip of the size press is very brief, and consequently, the operation must be carefully controlled to ensure that the requisite amount of solids is absorbed uniformly across the sheet. At the same time, the amount of

water absorption should be minimized so that the stream requirement for subsequent drying is maintained at the lowest level.

There are two basic mechanisms for incorporating starch solutions into the sheet at the size press. The first one is the ability of the sheet at the size press; the second one is the amount of solution film passing through the nip and the manner in which the paper and roll surfaces separate. Factors that favor greater absorption are low solution viscosity, high solution temperature, low machine speed, high sheet moisture, high sheet porosity, and low level of internal sizing. The factors favoring greater film thickness include high sheet roughness and low nip pressure.

Although the wood fiber sizing treatments can resist penetration by fluids and increase the hydrophobicity of wood fiber based products, the water proof efficiency is not high enough for food and drink package applications.

1.2 The Use of Barrier Coating on Paper/Linerboard Surface

Wood fiber based substrates such as paper, are widely used in packaging operations. Paper, however, has a very poor resistance to penetration by water vapor, gases, oil, solvents, and greases. To improve the water vapor barrier resistance, paper has been coated with a variety of substances. Barrier coating is one of the most important approaches for manufacturing high water resistance wood fiber containers. The most common paper coating is wax. While wax coated paper has good water vapor barrier resistance in a smooth or uncreased condition, it has poor resistance after it is ceased. Apparently the brittleness of the wax is so great that ceasing causes it to fracture and break thereby providing many areas through which water vapor can pass with little or no resistance.

1.2.1 The Use of Coater in Barrier Coating

Barrier coating operations can be applied on-machine or off-machine. Strong arguments can be made for each method, and debate continues within the industry as to the relative merits and cost-effectiveness of the two approaches. Generally, on-machine coating is most feasible where the application is light to moderate and the quality requirements are not too exacting. The barrier coatings are usually applied off-machine as part of a converting operation.

The barrier coatings can be applied by single-sided coaters, as well as a good selection of equipment for simultaneous two-sided application. Some paper products require coating only on one side of the sheet; a one-sided application is generally easier to control and simplifies the subsequent drying operation. Many two-sided coated grades are produced utilizing two coating stations with dryers in between. A wide variety of equipment is used to apply barrier coating. The major kinds of coaters used in the industries are introduced as follows.

Massey Print Roll Coater

The first on-machine coating is carried out using equipment adapted from the size press. In the Massey print roll coater, the rolls that smooth out the coating mixture and spread it evenly by the time it reaches the two large applicator rolls. Typically, one or more of the metering rolls oscillate. The pressure is varied between rolls to control the amount of coating transferred.

Air-Knife Coater

In the air-knife coater, the sheet picks up the coating mixture from an applicator roll running in a trough. The sheet then passes over a backing roll, where a sharp jet of

air impinges on the sheet, evening out the coating layer and blowing off the excess. In the design, it is vital that the air jet be oriented at the correct angle and be of uniform intensity across the entire width of the machine.

Rod Coater

For the rod coater, the sheet picks up the coating mixture from an applicator roll. Here, the doctoring and smoothing function is performed by a small diameter roll or wire wound rod which rotates in the opposite direction to the travel of the web. Since web tension is used to maintain pressure against the rod, this coating method is generally limited to heavier weight products that can withstand the tensile loading.

Blade Coater

Since their introduction in the 1950s, blade coaters have undergone extensive development, and a large number of designs are currently being employed. In all cases, the web is given a generous application of coating mixture, and the excess is removed by using a metal blade. In some designs, the blade tip is beveled at the same angle as the blade orientation; and the tip rides on a thin film of coating and performs the metering and smoothing function. In other designs, the blade is very thin and is flexed against the web. Generally, the so-called bent-blade designs allow higher coat weights and are less prone toward scratching. In all cases, the angle and pressure of the blade against the metal or rubber-covered backing roll determine the weight of coating retained by the sheet.

Puddle Coater

One of the earliest blade coaters was the pond or puddle coater. In more recent designs, the blade is separate from the applicator, leading to the designation of trailing blade coater. Recent variants are the inverted coater and the vacuum blade coater. Designs which coat both sides at the same time are the Billbalde coater and the opposed-blade coater.

Cast Coater

A specialized off-machine technique known as cast coating is used to produce paper of exceptional gloss and smoothness. Here the wet coated paper is pressed into contact with a large-diameter, highly-glazed cylinder during the drying phase. Great care must be taken at all steps of the process. The base sheet must be fairly porous so that water vapor given off during the drying of the coating can pass through it. The binder must have the ability to adhere to the hot chrome surface when wet, and then when dry, to separate without picking or plucking.

Extrusion Coater

The extrusion coater is used primarily for plastic coatings. Here, the heated resin is extruded through a slot as a hot viscous film which is combined with the paper between a pair of rolls. The combining operation takes place so rapidly that a permanent bond is created between the plastic film and the paper. A group of barrier coatings known as hot melt coatings have gained wide acceptance in recent years. These coatings consist of mixtures of polyolefins and wax-like materials that have excellent barrier properties at low thickness levels. Hot melts are usually too viscous for conventional coater equipment, but not viscous enough for the extrusion coater. Consequently, special

equipment has been developed, such as the curtain coating is pumped into the die slot from which it is discharged vertically downward in the form of a falling film or curtain. The sheet is passed through the curtain at high speed and the coating is deposited directly on the surface, where it solidified by cooling.

1.2.2 The Use of Chemicals in Barrier Coating

In the 1800s, animal glue was widely used as an adhesive in paper coatings. In the 1900s, animal glue was largely replaced by casein. Casein, used initially in the halftone printing process, forms a tough film and can be treated with formaldehyde to provide water resistance [1,2]. Casein is used in many high quality coatings for offset printing where water resistance, high gloss, and toughness of surface is desired. A wide variety of chemicals are used to apply barrier coating. The major kinds of chemicals used in the industries are introduced as follows.

Starch and Modified Starch Coating

In the 1900s, it was found that starch and modified starches can be used in a wide range of applications for coated paper in the low cost publication field where water resistance is a major requirement. Huang and co-workers reported that the starch in coatings applied to paper or paperboard, used in packaging detergents containing a persalt, is treated with a cross-linking agent to prevent water penetration and discoloration of the paper and paperboard due to oxidative degradation of carbohydrate materials to colored products [3-5]. The cross-linking agent serves to tie up functional groups of the carbohydrate materials such as cellulose in the paperboard and starch materials on and in the paperboard which may otherwise be oxidized by the release of

hydrogen peroxide from the persalt. The preferred cross-linking agents are melamine-formaldehyde and urea- formaldehyde resins.

In some applications, Kelly and co-workers reported that starch could be cross-linked using urea or glyoxal to impart water proofing properties [6-7]. Paper coating compositions are provided containing urea or glyoxal, starch as a binder. Exemplary of these compositions is a fluid dispersion of clay in aqueous medium containing starch and form about 2 to 10 % based on the weight of the starch of a latent insolubilizer for the starch. The latent insolubilizer is the reaction product of urea and glyoxal at a mole ration of from about 0.5 to 0.75 mol of urea to 1.0 mol of glyoxal. These compositions cure at low temperature, are stable, and provide coatings which possess high water resistance.

Water-Soluble Polyvinyl Alcohol Emulsion Coating

In the 1970s, many synthetic water-based systems had been developed. Polyvinyl alcohol provides strong durable coatings with good optical properties. Many researches and development activities had been devoted to emulsion type coatings [8,9]. Emulsions are low viscosity systems affording high solids content, easy handling, and less water to evaporate in the dryers than with the common natural binders. Increased gloss, better ink holdout, improved water resistance, and more flexibility are also obtained with these emulsion systems which are commonly used in combination with starch and casein.

It also has found that the water resistance, especially resistance to hot water, low moisture absorption, and good fatness to washing of water-soluble PVA containing paper having water-dissolving temperature of 95 ^{o}C or below can be remarkable improved by treating the paper below 40 ^{o}C with a solution which has been prepared by the addition of

titanium tetrachloride to water, or a solution made by dissolving in a mineral acid precipitate which has been prepared by adding titanium tetrachloride to water, and then adding ammonia [10].

Styrene-Butadiene Latex Coating

In the 1970s, Braidich and co-workers reported that an improved latex paper coating composition was found by taking the latex of a copolymer prepared from a substitute or unsubstituted mono-vinyl aromatic hydrocarbon monomer, an aliphatic conjugated diene hydrocarbon monomer and an unsaturated monomer or dicarboxylic acid monomer, reacting most of the carboxyl groups in the copolymer with an epoxide after the latex preparation, then mixing the resulting latex with another colloidal water-dispersible polymer and other coating ingredients to yield an improved paper coating composition [11]. That is, the use of a modified carboxylated polymer latex wherein a large percentage of the carboxyl groups are modified to a nonionic form results in a latex having improved compatibility with both the other colloidal water-dispersible polymer and filler, and having a sought-after characteristic of high water resistance as well as cross-linking ability.

Styrene-butadiene, primarily used in publication grade papers, was the first successful emulsion type product used in paper coating [12]. The improved carboxylic latex is produced by copolymerizing in an emulsion system comprising a synthetic emulsifier. Chich and co-workers found that improved paper coating compositions could be prepared from a latex composition comprising a mixture of styrene and butadiene [13,14]. The latex paper coating which has good porosity to permit rapid drying without blistering and resistance to water and moisture during the coating process.

Acrylic Latex Coating

Acrylics are commonly used as coatings on paperboard for food packaging due to their water resistance and low residual odor. High gloss and good ink holdout are typical properties of the acrylics which contribute to print quality in these relatively expensive coatings. The paper coating compositions containing, as binder, mixtures of (a) emulsion polymers of major amounts of mono-vinyl aromatic monomers, (b) emulsion polymers of major amounts of acrylates or methacrylate, and (c) emulsion polymers prepared in two stages from mono-vinyl aromatic monomers and acrylates or methacrylates. These compositions are particularly suitable for the manufacture of art paper if the amounts of polymerized units of mono-vinyl aromatic monomers and acrylates or methacrylates in the polymers (a), (b), and (c) together are such that a random copolymer containing the quantities of these monomers has a glass temperature of between -20 ^{o}C and 30 ^{o}C [15].

Polyethylene and Ethylene Copolymer Coating

Polyvinyl acetate provides good moisture resistance, good grease resistance, and responds well to calendaring operations to produce a glossy surface. For food containers, a number of barrier coatings have been developed, including polyethylene [16], microcrystalline wax [17], and ethylene-vinyl acetate copolymers [18]. In general, these materials improve the durability and film strength, raise the softening point, and increase the gloss and heat-seal properties.

Polyvinylidene Chloride Emulsion Coating

In the 1980s, polyvinylidene chloride emulsion coatings with the capability to provide high solids systems of minimum viscosity with excellent barrier properties was found by Demol and co-workers [19]. The coating for supports which confers to such

supports a high impermeability to water, water vapor, gases, greases, oils, etc., can be produces by employing at least 2 copolymers of vinylidene, which copolymers have different compositions and natures. The use of water-based coating, hot melts, and for some specialty uses solvent-based vehicles for paper coating continues to be an area of extensive research and development activity as systems are developed to meet the increasingly restrictive demands of pollution control, health regulations, and energy consumption.

Polyolefin Coating

In the 1990s, a water resistant corrugated paperboard material was prepared wherein the paperboard components were each coated on both sides with a thermoplastic polyolefin film which acted as a water barrier and a water resistant adhesive for bonding the components together. The corrugated medium is also pretreated with an internal size treatment to prevent edge wicking, and for the purpose of corrugating rolls are preheated to a temperature slightly less than the melting point of the thermoplastic polyolefin film while a lubricating material is simultaneously applied to either the corrugating rolls or the medium at the corrugating nip [20].

Thus it may be stated that the novelty in the process as regards the product produced lies in the use of thermoplastic polyolefin coating of at least 20 μm thick on both sides of both the medium and the linerboard, in combination with a surface treatment to the corrugating medium. Since corrugating medium is normally untreated, to enable the medium to pick up the usual starch adhesive when forming conventional corrugated paperboard, the mere fact of applying a surface treatment to the corrugating

medium itself, according to the process represents a departure from the conventional manufacture of corrugated paperboard.

Recently, with regard to the barrier coating layer formation, a wide range of other candidates are available, such as nanocomposites [21,22], ceramics [23], metals [24], and sol-gel coating layers [25,26], etc.. The conventional barrier has been developed based on the extrusion products of a range of polymers, such as wax, polyethylene, and poly(ethyl terephthalate) [27,28], etc..

1.2.3 The Drying of Barrier Coatings

Drying of the barrier coating also plays another important role in preparing water-proofing paper products. Sometimes, conventional steam cylinder methods are used for the drying of coatings. More often, other methods must be used to avoid disturbing the coating film. The two methods employed most often are hot air impingement and infra-red drying.

High-velocity convective hoods placed over conventional steam cylinders are a popular method of drying single sided coatings. Tunnel-drying is another approach, suitable for both single and double coated sheets. In the method, the air temperature is controlled to suit the drying requirements and speed of the machine, while the paper is carried through the tunnel on rollers, supported on foils, or held up by air impingement. A complete on-machine coating system consisting of two single-sided coated stations followed their respective dryers. Off-machine coating system is similar to on-machine one.

An infra-red emitter (usually gas-fired) provides a compact, high-intensity heat source which transfers its energy without any physical contact, ideal for the drying of

coatings. However, since the infra-red radiation unit supplies only a source of heat, air must also be provided to carry away the moisture evaporated from the coatings. Some drying units, therefore, combine infra-red and air-impingement principles for more efficient operation.

1.2.4 The Surface Properties of Coated Paper

The surface properties of the raw stock influence the formation of the coated layer in two ways. Surface roughness has a significant impact on the coating thickness uniformity; while surface absorptivity determines the composition of the actual coating layer. When the coating first contacts the paper surface, capillary forces within the sheet structure cause a movement of water-soluble components into the smaller pores of the sheet, leaving behind at the surface (by filtration action) a formulation richer in pigment particles.

The type and amount of binder in the coating formulation has a pronounced effect on coating structure because it influences the rate of fluid penetration into the raw stock, the degree of filling between pigment particles, and the rate of drying. The basic structure of the coating layer is more fundamentally related to the size and shape of the pigment particles, and the degree of packing. Additives in the coating mix will normally determine the flexibility of the dried adhesive and the subsequent reorientation of pigment particles during supercalendering.

The air-knife coater tends to deposit a uniform layer that follows the contours of the base sheet. The roll coater provides good coverage, but patterning defect are introduced from the film-splitting. Blade coating results in good filling in the surface valleys, but the uniformity of coating layer thickness is sacrificed to obtain increased

smoothness. Each coating process forms a somewhat different layer; hence, some coating operations employ multiple coating steps to combine the advantages of two or more methods.

The effects of drying conditions on coating structure can be significant. If the coating dries too quickly, those areas with a thicker deposit or a slower rate of absorption will retain a higher proportion of adhesive. And thereby yield a different coating structure. As the speed of the coating operation increases, and the time interval between application and drying becomes shorter, this problem can be more severe.

During drying, a considerable amount of shrinkage occurs in the thickness of the coating layer. The extent of shrinkage is mainly a function of the solids content of the initial dispersion, but is also affected by the shape of the pigment, the degree of dispersion, and the physical properties of the binder. The shrinkage is undesirable because a portion of the original sheet roughness returns, this problem is most severe with low coat weights.

Supercalendering is often carried out on coated sheets to compact the coating structure and develop a greater level of smoothness. If the coating structure is not uniform, it is likely that the supercalendering will further emphasize the non-uniformity. Areas of the coating structure relatively rich in adhesive will not develop as high a gloss as adjacent areas, and the sheet will exhibit a finely-mottled appearance.

Coating clays are a laminar form of clay. When the coating is initially applied, the clay platelets are randomly oriented. To produce a glossy appearance, a substantial number of these tiny platelets must be oriented more nearly parallel to the plane of the sheet. At high supercalendering pressures, this reorientation occurs while the binder is

squeezed through the pigment particles. Light reflection from the supercalendered surface is more specular, thus improving gloss; however, low areas are not affected.

The common objective with barrier coatings is to provide a barrier to water, water vapor, air, or grease. Although wax and hydrophobic polymers can be used to produce high water resistance packages for food and medical applications, the thick coating layer (>30 μm) results in high coating cost and poor recyclability. Furthermore, the water-repellent and decomposable products obtained by regular wax or polymer coating can not greatly benefit customers and industries.

1.3 Properties and Applications of Superhydrophobic Surface

The common way for enhancing the surface hydrophobicity is lowering the surface energy. However, even materials with the lowest surface energy (6.7 mJ/m^2 for a surface with regularly aligned closest-hexagonal-packed —CF_3 groups) gives a water contact angle of only around 120^o. In fact, ultra hydrophobic surfaces with water contact angle greater than 150^o may be developed only by introducing proper roughness on materials boundary with low surface energy.

In some Eastern cultures, the lotus plant is a symbol of purity. Although lotuses prefer to grow in muddy rivers and lakes, the leaves remain clean. It is found that lotus leaves have a natural cleaning mechanism. The water droplets roll off lotus leaf surfaces like mercury, taking dust particles, tiny insects, and surface contaminants with them. This self-cleaning property is caused by both the hierarchical roughness of the leaf surface from micrometer-sized papilla with protrusions and the intrinsic material hydrophobicity of a surface layer of epicuticular wax covering these papilla. The epicuticula wax provides the low surface energy, and the papillae structure brings a large

extent of air trapping when contacting with water. With a very rough and heterogeneous papillae structure, the surface allows air to be trapped more easily underneath the water droplets, so the droplets essentially rest on a layer of air. Rather, a significantly higher surface area compared to the projected area creates a greater energy barrier of liquid-solid interface. Coupled to this, when the surface energy of the surface material is intrinsically low, the combined effect is the surface will repel any water that comes into contact with it.

Borrowing from the character of lotus leave surface, a simple method to prepare synthetic coatings with exceptional anti-wetting properties is developed. The ability to fabricate water-repellent surface has attracted great interest due to the potential use in various applications, such as self-cleaning facades, self-cleaning window panes, self-cleaning toilet, and self-cleaning kitchen utensil. Besides, it can help with highly reducing drag on ship hulls, motor vehicles, and aircrafts to save energy and increase the speed of vehicle. Self-cleaning fabrics could revolutionize the apparel industry. The technology can be used to create t-shirts and underwear that can be worn hygienically for weeks without washing. The new technology attaches nano-structures to clothing. Then, chemicals that can repel water, oil, and bacteria are directly bound to the nano-structures. These two elements combine to create a protective coating on the fibers of clothing. This self-cleaning clothing both prevents the attachment of dirt and bacteria, and forces liquids to bead and run off [29-33].

Superhydrophobic surfaces indicate the surfaces with water contact angle larger than 150^{o}. Compared with hydrophobic surfaces, superhydrophobic surfaces are with much higher anti-wetting property and better self-cleaning property. Superhydrophobic

surfaces are usually prepared by combining an appropriate surface roughness with a hydrophobic material, since the hydrophobicity of a surface is determined by its chemical composition and topography. There have been numerous recent reports about successful generation of polymeric and inorganic superhydrophobic surfaces utilizing various surface treatment techniques:

Lithographic Patterning

Lithographic patterning is a process used to selectively remove parts of the substrate surface to produce roughness on the surface. The process is used to transfer the patterns of the masks onto the substrates. After irradiation, the substrates are etching using laser, X-ray, or chemicals as shown in Figure 1.1. When the etching process is complete, the patterned substrates are cleaned follow with surface modifications [29,30]. Lithographic patterning is an efficient method to prepare superhydrophobic surfaces on silicon wafers and metal substrates because it affords exact control over the shape and size of the objects it creates, but the process damages the wood fiber substrates, which is a significant disadvantage for this method. Furthermore, the process is very expensive that is difficult to be applied to large scale commercial production. However, the lithographic technique can produce permanent surface roughness, which has certain advantage than other techniques.

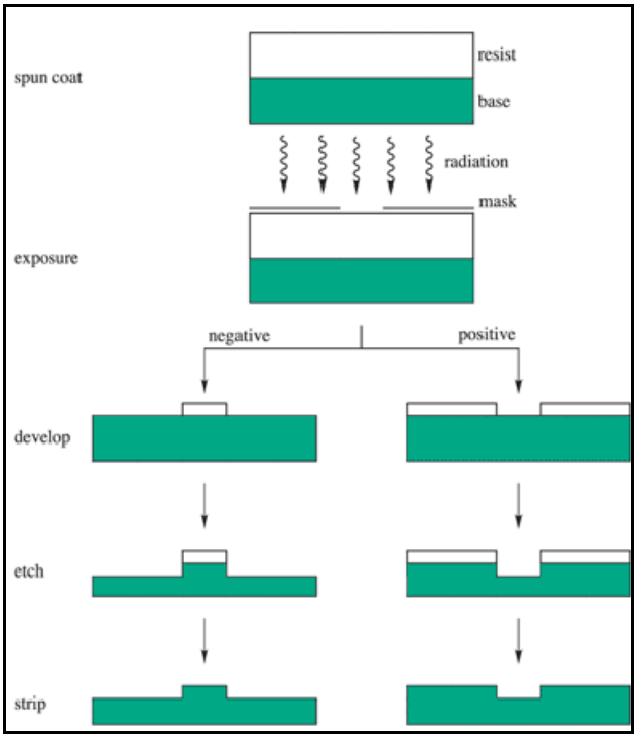

Figure 1.1 Schematic representation of the lithographic patterning process.

Laser/ Plasma Etching

Etching is the process of using strong acid, laser, or plasma to cut into the unprotected parts of a substrate surface to create a design in intaglio in the substrate and increase the surface roughness. In the plasma etching processes now routinely used to fabricate superhydrophobic surface, a mask is used to define an area to be etched, and a glow discharge generates reactive species which etch the exposed area as shown in Figure 1.2 [31]. Depending on the myriad process parameters, such as gas components, gas pressure, and of discharge power and frequency, the etch can have varying amounts of selectivity, anisotropy, and damage. In addition, the requirement of having a mask previously applied to define the etch pattern greatly increases the complexity of the processing sequence and can lead to problems with yield and throughput.

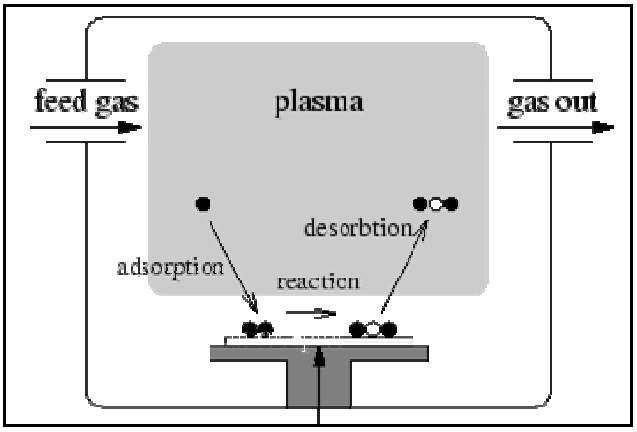

Figure 1.2 Schematic illustration of the plasma etching.

In other researches, laser light has been used to control the etching rates [32,33]. The laser etching process is illustrated with Figure 1.3. Various light-assisted processes have been studied, including those relying on gas and surface phase interactions. The laser is also found to inhibit polymer deposition on the surface. The possibility of maskless etching is also demonstrated. In addition, by etching using the laser without the discharge, a higher surface roughness of the underlying etch process has been obtained.

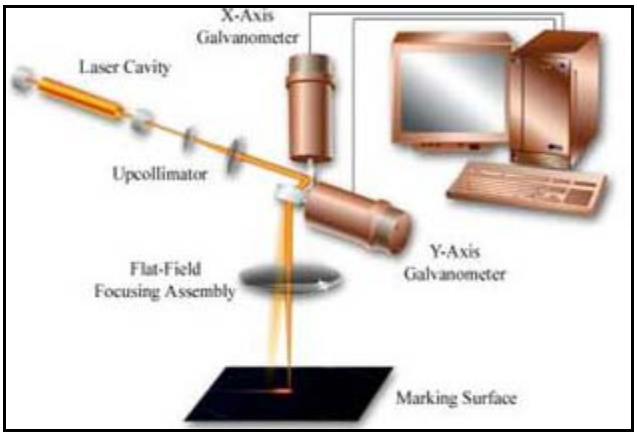

Figure 1.3 Schematic illustration of the laser etching.

Vertical Alignment of Nanotubes/ Nanofibers

The purpose of attaching vertical aligned nanotubes/ nanofibers to the substrate surface is to decrease the fraction of solid surface in contact with water droplet, and to increase the fraction of air surface in contact with water droplet, respectively [34-37]. This substrate surface allows air to be trapped more easily underneath water droplets, and increases the hydrophobicity of surface. The fabrication procedure is shown in a Figure 1.4. A porous template of commercial alumina membranes with pores, where porosity consists of an array of parallel and straight channels, is in contact with a polymeric solution, and a thin polymer layers cover the pore walls of the membranes in the initial stage of wetting. After a period of time, the template is dissolved away by sodium hydroxide solution at room temperature, and an aligned polymeric nanotube/ nanofiber layer is obtained. The method used to fabricate polymeric nanotube/ nanofiber layer is simple and reproducible.

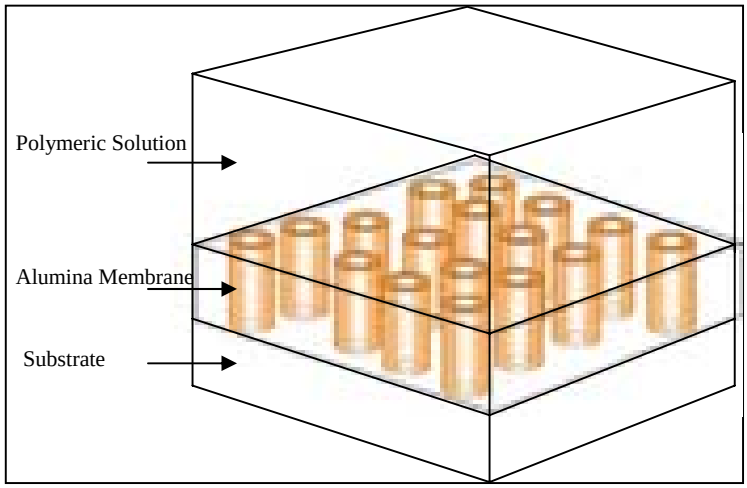

Figure 1.4 Schematic illustration of vertical alignment of nanofibers.

Sol-Gel Method

The sol-gel process is a wet-chemical technique used for the fabrication of materials starting either from a chemical solution or colloidal particles (sol) to produce an integrated network (gel). Recently, the researches are working on depositing sol on a substrate to form a layer of porous film by dip-coating or spin-coating in order to increase the surface roughness [38-40] as shown in Figure 1.5. Sol-gel processing includes two approaches, hydrolysis of metal alkoxides and polycondensation of hydrolyzed intermediates. Most of the interest in this method is concentrated on metal organic alkoxides since they can form an oxide network in organic matrices. This process provides a method for the preparation of inorganic metal oxides porous structures under mild conditions starting from organic metal alkoxides. This permits structural variations without compositional alteration. The sol-gel approach is interested in that it is a low-temperature technique that allows for the fine control on the product's chemical composition. However, the formation of a cross-linking network of organic metal oxides makes a component difficult to process, and it is a disadvantage that circumscribed the application of this method.

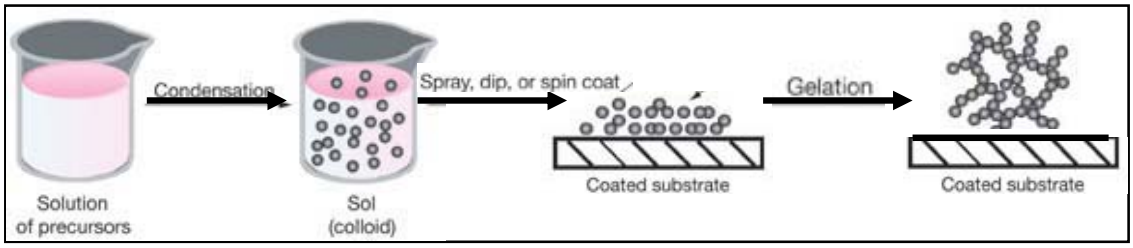

Figure 1.5 Schematic representation of the sol-gel method.

Phase Separation

A superhydrophobic polymeric surface with a high water contact angle and low sliding angle was facilely created by a one-step polymer solution casting method [41,42]. The superhydrophobicity was resulted from vapor-induced phase separation without modification with special low surface energy compounds. It is well known that polymer solution becomes thermodynamically unstable when evaporating the solvent under certain conditions after casting. As a result, phase separation will occur to form a polymer rich phase and a polymer poor phase. The concentrated phase solidifies after phase separation and forms the matrix, whereas the polymer poor phase forms the pores. This method can be extended to a variety of polymers to fabricate the superhydrophobic surface through a selection of suitable solvent and nonsolvent vapor. The facility and economy of this method make it suitable for the practical application of superhydrophobic surface in large area.

Binary Colloidal Assembly

Binary colloidal assembly method is a technique used for the fabrication of surface roughness by colloidal self-assembling. Monodisperse colloidal spheres usually self-assemble into highly ordered hexagonal or cubic close-packing arrays. Due to their long-range ordered structures, colloidal self-assemblies can be employed to pattern substrates. In this procedure, irregular structures with a hierarchical roughness surfaces were derived from binary colloidal assemblies as shown in Figure 1.6 [43]. Inorganic particle-loaded hydrogel spheres and polymers were consecutively dip-coated on substrate surface. The former assemblies were recruited as templates for the latter self-assembly. Due to the hydrophilicity difference between substrates and inorganic particle-

loaded hydrogel spheres, the region selective localization of polymer spheres leads to irregular binary structures with a hierarchical roughness. The subsequent modification with low surface energy molecules yields a superhydrophobic surface. The heating treatment can largely enhance the mechanical stability of the resulting binary structures, which allows regeneration of the surface superhydrophobicity, providing a good durability in practice.

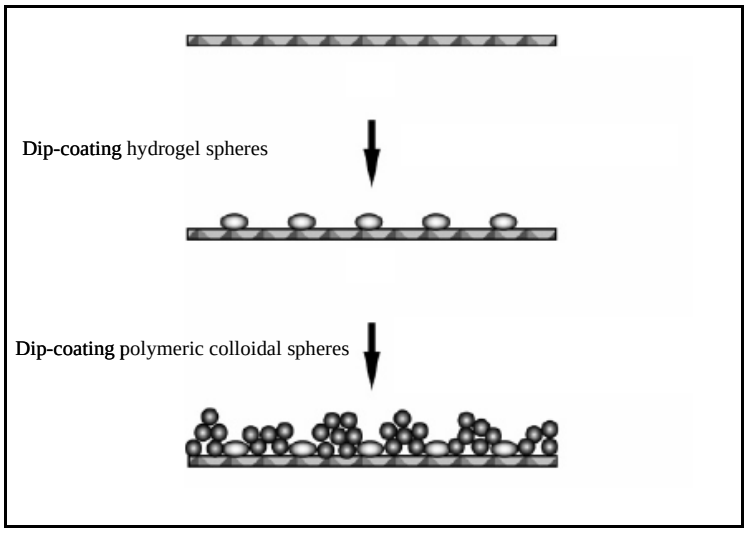

Figure 1.6 Schematic representation of the binary colloidal assembly.

Glancing Angle Deposition

Figure 1.7 shows the glancing angle deposition (GLAD) method, the extreme accentuation of atomic shadowing that occurs when the impinging vapor flux arrives at the substrate from near-glancing angles results in the nanostructure, high porosity, and large surface area of GLAD films. GLAD is a straightforward method for fabricating nano-structured thin films of isolated columnar structures that can be sculpted into a variety of structural motifs including slanted posts, helices, and vertical posts [44-48]. The experimental control over film structure arises because film growth will always tend

toward the source flux. The GLAD apparatus provides control over the angle at which the source flux arrives at the substrate. Under these conditions, vapor flux arriving at oblique angles at the substrate results in slanted post structured films. Following this reasoning, various film structures can be prepared by rotating the substrate about the axis normal to the substrate surface during deposition.

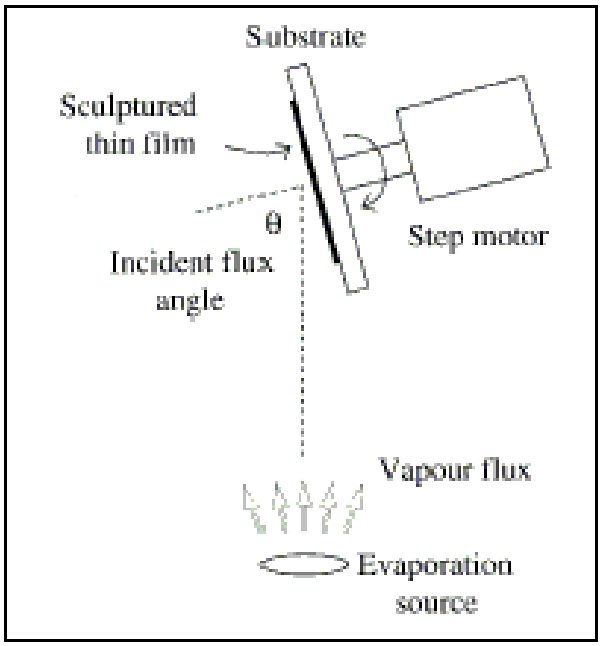

Figure 1.7 Schematic representation of the glancing angle deposition.

Undoubtedly, low-coast, superhydrophobic, water-repellant, and self-cleaning fibers can bring a large number of benefits to the paper industry, food package industry, and medical supplying industry. The superhydrophobic paper packages can also be extremely important when suits protective against chemical and biological weapon are designed. It is clear that superhydrophobic fibers and lotus-like substrates will revolutionize and extend the capability of many paper-based applications as well as create new products markets. They are ideal products for food packages, biomedical applications, electronic resistant papers, and antibacterial papers. The biodegradable

paper products can be extremely interested by military and homeland security applications. However, to the best of our knowledge, a simple and inexpensive way to prepare wood-fiber materials demonstrating the lotus effect have not yet been created.

Layer-by-layer (LbL) assembly technology, which is developed by Decher and co-workers [49], has been proven to be a simple and inexpensive way to fabricate various kinds of surfaces with tailored chemical deposition and architecture in micro-scales and nano-scales [50-53]. Recently, there have been several reports concerning the use of LbL assembly technique to construct superhydrophobic surfaces [54-59]. Shiratori and co-workers construct superhydrophobic surfaces by first fabricating a LbL assembled hybrid film of polyelectrolyte/ silica nanoparticles and then removing the organic components by calcination at 650 ^{o}C to develop an inorganic nanostructure for superhydrophobic behavior [54]. Zhang and co-workers report the use of polyelectrolyte multilayer as a performed matrix for electrochemical deposition of gold and silver clusters to fabricate superhydrophobic surfaces [55]. Rubner and co-workers mimic the superhydrophobic behavior of the lotus-leaf structure by first treating a 5-bilayer poly(allylamine hydrochloride) (PAH)/ poly(acrylic acid) (PAA) film in acidic solution to induce microporous structure follow by coating the micorporous surface with silica particles [56]. Cho and co-workers fabricate the superhydrophobic surface by depositing silica nanoparticles on the surface of a 10-bilayer PAA coated ZrO_2 nanoparticles/ PAH film follow with a simple fluorination [57]. Schlenoff and co-workers prepare superhydrophobic surfaces by a LbL assembly of fluorinated polyelectrolytes and natural nano-rods [58]. Taking advantage of the amplified exponential growth of PAA and polyethylenimine (PEI) in the presence of silver ions, Ji and co-workers report a way to

construct PAA/ PEI-Ag^+ films with hierarchical micro- and nanostructures for use as superhydrophobic surface after thermally crosslinking the film [59]. The above results, as well as the easy fabrication of large area films with LbL assembly technique holds great promise in fabricating superhydrophobic surfaces in a simple and inexpensive way. The assembly technology also enables the deposition of multilayer films on non-flat surfaces [60-62].

This study focuses on developing a simple and inexpensive way to prepare superhydrophobic paper products. In this study, superhydrophobic paper products are developed by layer-by-layer deposition follow with a fluorination treatment. The resistance to moisture and water is investigated as a function of relative humidity. The characters of surfaces with different roughness are also studied. It is expected that the superhydrophobic paper products should have super resistance to water, oil, and all contaminations.

1.4 Superhydrophobic Theoretical Background

A surface having a water contact angle greater than 150^o is called a superhydrophobic surface. A droplet of water easily rolls off a surface having such excellent hydrophobicity. Hence, Superhydrophobicity is defined by two criteria: a very high water contact angle and a very low sliding angle. The sliding angle is the inclination angle of the surface from horizontal at which a water droplet completely rolls off the solid surface. In general, contact angles are measured for the evaluation of the surface tension and wettability. Although it is hard to measure the surface tension of a solid directly, it is easy to measure the its contact angles.

When a liquid droplet is placed on a homogeneous smooth solid surface, the contact angle, θ, can be obtained using Young's equation [63]:

$$\cos\theta = \frac{\gamma_{sv} - \gamma_{sl}}{\gamma_{lv}}$$

where γ_{sv}, γ_{sl}, and γ_{lv} are the interfacial tensions of the solid-vapor, solid-liquid, and liquid-vapor phases, respectively.

Wenzel modified Young's equation and proposed a well known equation for the contact angle of liquids on a rough homogeneous surface, θ_w, which is as follows:

$$\cos\theta_w = r(\frac{\gamma_{sv} - \gamma_{sl}}{\gamma_{lv}}) = r\cos\theta$$

where r is the roughness factor defined as the ratio of the actual surface area of the rough surface to the geometric projected area. This equation implies that when the intrinsic contact angle of a liquid on a rough solid surface is larger (smaller) than 90^o, the surface will become superhydrophobic (superhydrophilic) because *r* is always larger than 1 [64]. However, it should be noted that the morphology of the surface has a significant influence on the observed contact angle for rough surfaces. Roughness, in simple terms, by itself can not explain the high hydrophobicity of very rough surfaces, and Wenzel's equation is not necessarily applicable (depending on the *r* value, Wenzel's equation will become inapplicable to calculate θ_w as $r\cos\theta > 1$). For very rough surfaces, a composite surface structure made of air (trapped in undulations of a rough surface) and the primary surface material are often observed. The wetting for such heterogeneous surfaces is traditionally described by the Cassie's equation [65]:

$$\cos\theta_c = f_1\cos\theta_1 + f_2\cos\theta_2$$

where θ_c is the Cassie contact angle; f_1 and f_2 are the fractions of materials 1 and 2 on the surface, respectively. Angles θ_1 and θ_2 represent the intrinsic contact angles of the liquid with materials 1 and 2 that can be found from Young's equation. Cassie's equation can be rewritten as follows where the contact angle of liquid with air is considered to be 180^o (θ is the intrinsic contact angle for the primary surface material):

$$\cos\theta_c = f(\cos\theta + 1) - 1$$

where f is the fraction of the solid surface in contact with liquid; the fraction of air (trapped in the surface roughness) in contact with liquid at the surface is $1 - f$. The modified Cassie's equation can be used to calculate the fraction of the air pockets at the surface.

Quéré and co-workers studied rough hydrophobic surfaces; the roughness had the form of fine microtextures with different geometries [66,67]. To understand the wetting behavior of such surfaces, they combined Wenzel's equation and the modified Cassie's equation to obtain the following equation for a liquid droplet on a solid substrate:

$$\cos\theta_{cr} = \frac{f - 1}{r - f}$$

In the equation, θ_{cr} is the critical intrinsic contact angle that delineates the wetting regime (Wenzel or Cassie). The equation shows that for $90^o < \theta < \theta_{cr}$, the Wenzel's mode is applicable although some cases have been observed with the metastable Cassie's mode [68]. For $\theta_{cr} < \theta < 120^o$, however, the Cassie's mode will be applicable because of the air pockets trapped below the liquid drop in the undulations of the rough surface. It should be noted that 120^o is the highest possible intrinsic contact angle for water on a surface obtained by lowering the surface energy.

CHAPTER 2

OBJECTIVES, APPROACHES, AND EXPERIMENTS

2.1 Research Objectives

It is well known that the roughness of hydrophobic surface enhances the surface hydrophobicity. The main tasks of the research are to develop the nano-structured roughness morphology on wood fiber or paper surface, followed by increasing the hydrophobicity of rough wood fiber surface by chemical modification, and to study the physical properties of the prepared superhydrophobic paper products. The objectives of the research are following:

1. Develop a method to control the nano-roughness of paper.
2. Chemically modify the surface from hydrophilic to hydrophobic.
3. Study the relation between coated particle size and surface hydrophobicity.
4. Prove the anti-contamination form biomaterials.
5. Study the feasibility of other particle coating methods.

The ultimate goal of the study is targeted to develop a novel nanomaterials and nanotechnologies to produce superhydrophobic paper products, for food industry, biomedical industry, military applications, and homeland security applications. In the study, both fundamental understanding and method development will be focused.

2.2 Materials

The silica particles with diameters of about 200 nm, 420 nm, 800 nm, and 1 micrometer were synthesized according to literature reported method [69]. The reagents used for silica particle synthesis, including tetraethyl orthosilicate (TEOS) (98%), ammonium hydroxide (NH_4OH) (28%), and ethanol (99.5%), were all purchased from Sigma-Aldrich. The top layer of commercial linerboard made from unbleached kraft softwood fiber was used as wood-fiber-based substrate. The aqueous solution of poly(diallyldimethylammonium chloride), Poly(DADMAC), with molecular weight of 100,000-200,000 (20 wt.% in water) was purchased from Sigma-Aldrich. 1H,1H,2H,2H-perfluorooctyltriethoxysilane (POTS) (97%), used for surface hydrophobic modification as shown in Figure 2.1, was purchased from Alfa Aesar. Deionized water purified in an ultrapure water system (NANOpure) was used in all the experiments. Escherichia coli-Ampicillin^R was used as model bacteria for antibacterial resistance test. Luria-Bertani (LB) medium used for growing and maintaining bacteria cultures were purchased from Sigma-Aldrich. Laboratory grade polystyrene (Mn=140,000; Mw=230,000) and tetrahydrofluoride (THF) (98%) used to study the effect of contact liquid viscosity were obtained from Sigma-Aldrich. All the chemicals were used as received. The Oji ACE-K-100 cationic starch powder was made by Oji Corn Starch Kabushiki Kaisha.

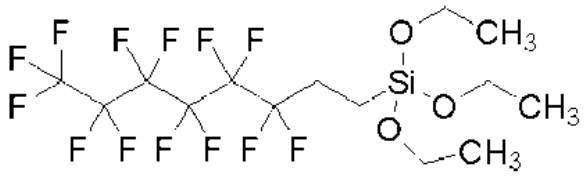

Figure 2.1 Molecular structure of 1H,1H,2H,2H-perfluorooctyltriethoxysilane.

2.3 Synthesis of Superhydrophobic Linerboard

2.3.1 Synthesis of Silica Particles

Silica particles were synthesized according to the process described by Stober et al.. In the process, TEOS was hydrolyzed to form silica particles in ethanol with a catalyst, NH_4OH, at room temperature as shown in Figure 2.2. Monodisperse spherical particles of controlled sizes, ranging from tens to thousands of nanometers, were synthesized in our lab by changing the concentrations of reactant and catalyst. A typical example of the synthesis is given below. In the synthesis of silica particles with an average diameter of 220 nm, TEOS (46.8 ml) was hydrolyzed to form silica particles in ethanol (300 ml) with the catalyst, NH_4OH (28.2 ml), at room temperature over a period of two days. Silica particles synthesized by the above method are hydrophilic, with hydroxide groups on the silica particle surface. Silica particles were then dried at room temperature and made ready for next step.

Hydrolysis:

$$Si(OR)_4 + H_2O \rightleftharpoons (HO)Si(OR)_3 + ROH$$

$$(HO)Si(OR)_3 + H_2O \rightleftharpoons (HO)_2Si(OR)_2 + ROH$$

$$(HO)_2Si(OR)_2 + H_2O \rightleftharpoons (HO)_3Si(OR) + ROH$$

$$(HO)_3Si(OR) + H_2O \rightleftharpoons Si(OH)_4 + ROH$$

Alcohol Condensation (Alcoxolation):

$$\equiv Si\text{-}OR + HO\text{-}Si\equiv \rightleftharpoons \equiv Si\text{-}O\text{-}Si\equiv + ROH$$

Water Condensation (Oxolation):

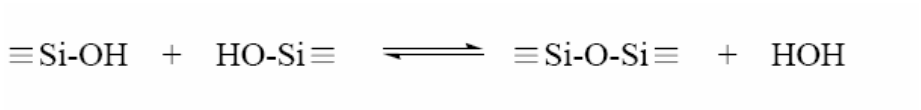

Net Reaction:

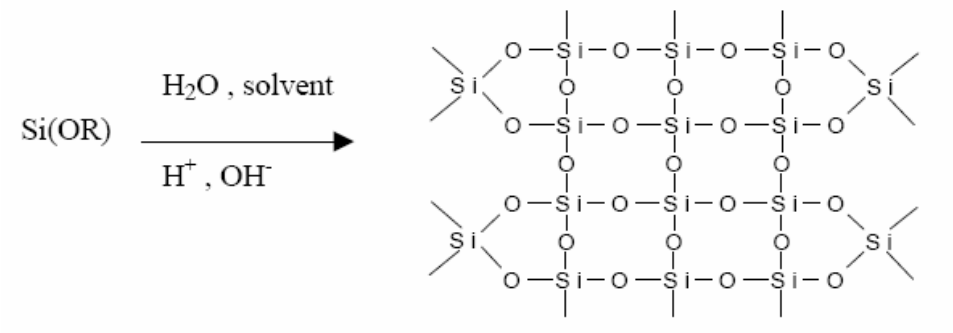

Figure 2.2 Synthesis of silica particles.

2.3.2 Preparation of Silica-coated Substrate

Cationic Poly(DADMAC) and anionic silica particles were used in layer-by-layer self-assembly deposition. First of all, 1 g of Poly(DADMAC) aqueous solution was dispersed in 19 g of deionized water. Secondly, 0.2 g of silica particles used for substrate coating was dispersed in 19.8 g of deionized water. Before usage, the silica suspension was sonicated by ultrasonicator (W-385) for 10 minutes to disperse the silica particles in the solution. The negative charged wood-fiber-based substrate was first immersed in prepared Poly(DADMAC) solution for 20 minutes to render the substrate positively charged, followed by rinsing with deionized water for 1 minute (Step A). The substrate was then immersed in silica solution for 10 minutes, followed by rinsed with deionized water for 1 minute (Step B). By repeating above steps, a multilayer film of Poly(DADMAC)/silica particles could be fabricated as shown in Figure 2.3.

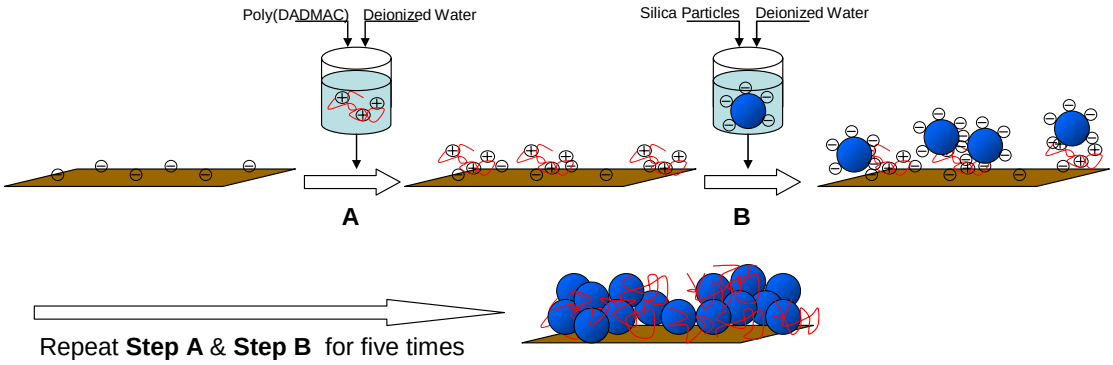

Figure 2.3 Schematic illustration of the fabrication of multilayer film assemble on linerboard surface.

2.3.3 Surface Modification of Silica-coated Substrate

The surface modification carried out by chemical vapor deposition of 1H,1H,2H,2H-perfluorooctyltriethoxysilane (POTS) was shown in Figure 2.4. The silica-coated substrate was placed in a sealed vessel, on the bottom of which was dispensed a smaller unsealed vessel within a small amount of POTS. The sealed vessel was then put in an oven at 125 °C to enable the silane group of POTS vapor to react the hydroxide group on the silica-coated substrate surface. After 2.5 hours, the substrate was removed to another clean sealed vessel and heated at 150 °C for another 2.5 hours to volatilize the unreacted POTS molecules on the substrate.

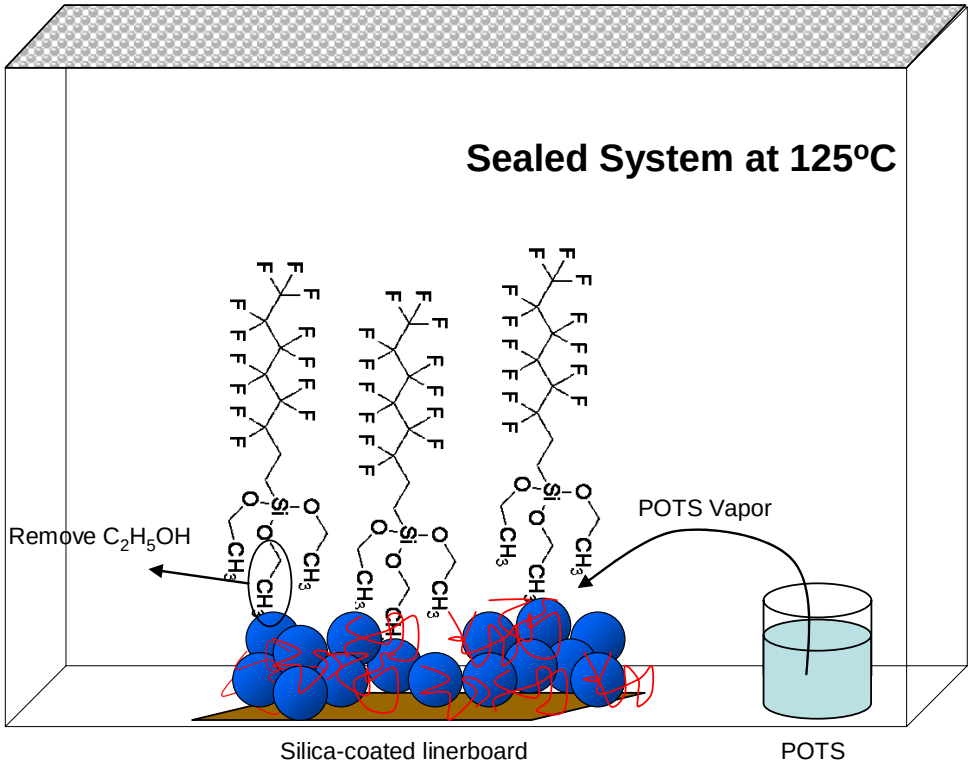

Figure 2.4 Schematic illustration of the surface modification on silica-coated linerboard surface.

2.4 Material Characterization Methods

The physical properties of the synthesized silica particles, silica-coated linerboard, and surface modified silica-coated linerboard were determined by a series of characterization methods as follows.

2.4.1 Scanning Electron Microscopy (SEM)

Hitachi 800 field emission scanning electron microscope and Leo 1530VP® field emission scanning electron microscope were employed to examine the surface morphology and microstructure of the polymer materials. The samples were stick to the top of the tape on the sample holder, and then fixed with compressed air. All the samples underwent a gold thin-film coating with BAL TEC MED 20 HR Sputtering Coater before the microscopic characterization. The coating was conducted at high vacuum ($<2x10^{-5}$ bar). All the microscopies are performed under 1kV, with a working distance range of 3 to 5mm.

2.4.2 Dynamic Contact Angle Analyzer (DCA)

Dynamic contact angle analyzer FTA200 (DCA) from First Ten Angstroms is designed to measure wetting phenomenon such as static or equilibrium contact angle, surface tension, surface energy, and absorption. The instrument features include a tilting heated stage and an APPRO BV-7105H black & white camera capable of taking 360 images per second. Standard substrates can be used to determine the surface tension of test liquids, and determine the surface energy of test solids. Measurements are made by observing the drop shape of a fluid that has been placed on substrate, using rapid video capture of images and automatic image analysis. Software included with the instrument can then use the image of liquid droplet shape to calculate static or equilibrium contact

angle. In the study, the water contact angles of the samples were measured at ambient temperature with a droplet volume of 0.013 ml.

2.4.3 Tensile Tester

Lab Master tensile tester (84-91 LTL) was employed to measure the tensile strength of the samples under different humidity conditions. The Lab Master tensile tester determines internal bond strength to 113 kg with 4.5 gram resolution and ±0.02% full scale accuracy. Peak force is measured by applying a force in the z-direction until separation occurs. All the samples were cut into specimens with a dimension of 15×7.25×0.4 mm^3. The specimens were held at 25^oC under different relative humidity for 12 hours before the tension strength measurements. The relative humidity was controlled by the amount of water in the sealed box as shown in Figure 2.5.

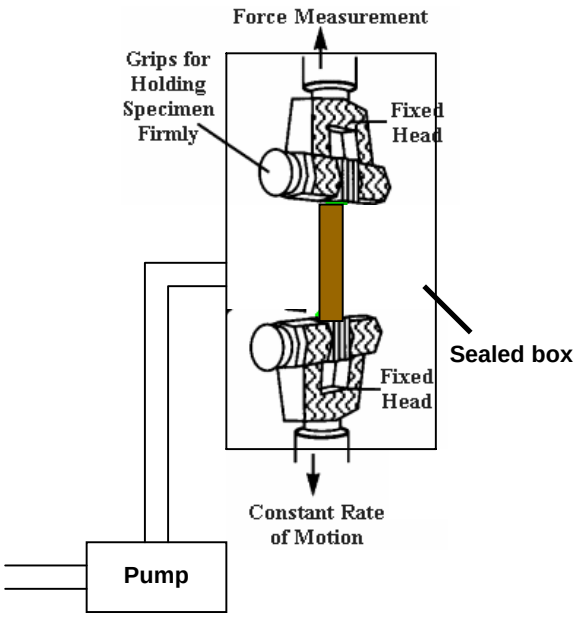

Figure 2.5 Schematic illustration of the tensile tester.

CHAPTER 3

RESULTS AND DISCUSSIONS

This study focuses on developing a simple and inexpensive way to prepare superhydrophobic paper products using layer-by-layer deposition method followed by a fluorination treatment. Three samples were prepared for the comparative study: linerboard (original linerboard paper), hydrophobic linerboard (the linerboard paper treated by POTS surface modification only), and superhydrophobic linerboard (the linerboard paper coated with silica particles followed by POTS surface modification).

The present chapter is divided into 3 sections. Section 3.1 presents the general characterization of superhydrophobic linerboard. Section 3.2 discusses the particle size effect of superhydrophobic linerboard surface. Section 3.3 introduces preparation of superhydrophobic linerboard with different methods.

Section 3.1 is divided into 8 sections. Section 3.1.1 presents the surface morphology of superhydrophobic surface from the SEM micrographs. Section 3.1.2 presents the hydrophobicity of superhydrophobic surface by measuring the water contact angles. Section 3.1.3 presents the surface roughness of superhydrophobic surface by developing a MATLAB program. Section 3.1.4 presents the moisture resistance of superhydrophobic surface with different relative humidity. Section 3.1.5 presents the tensile strength of superhydrophobic surface with different relative humidity. Section 3.1.6 presents the water resistance of superhydrophobic surface immersing in water. Section 3.1.7 presents the bacteria resistance of superhydrophobic surface by accounting

the CFU on the paper specimens after offering a sliding angle or immersing in water. Section 3.1.8 presents the silica particle size effect of superhydrophobic surface.

Section 3.2 is divided into 2 sections. Section 3.2.1 presents the surface roughness of superhydrophobic linerboard surface coated with different size of silica particles. Section 3.2.2 presents the surface roughness of superhydrophobic linerboard surface coated with different size ratio of mixed silica particles.

Section 3.3 is divided into 3 sections. Section 3.3.1 presents the preparation of superhydrophobic linerboard by spread-coating of silica solution followed by a fluorination treatment. Section 3.3.2 presents the preparation of superhydrophobic linerboard by dip-coating in cationic starch solution and silica solution followed by a fluorination treatment. Section 3.3.3 presents the preparation of superhydrophobic linerboard by directly synthesizing silica particles on surface followed by a fluorination treatment.

3.1 General Characterization of Superhydrophobic Linerboard

3.1.1 Surface Morphology of Superhydrophobic Linerboard

Silica particles were synthesized according to the process described by Stober et al. (1968). As show in Figure 3.1, the SEM micrograph of silica particles have an average diameter of 220 nm. Though slight agglomeration was observed in the micrograph, the particles dispersed very well in deionized water after applying ultrasonication.

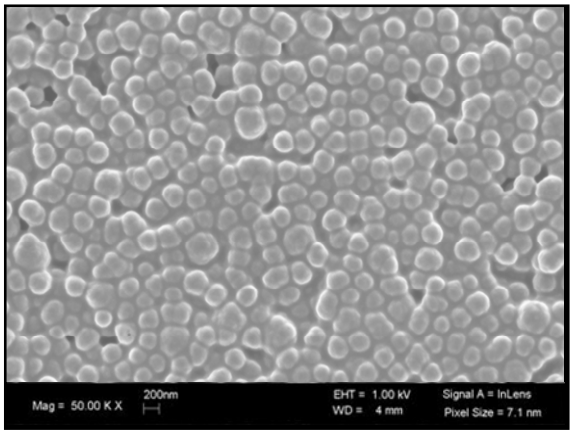

Figure 3.1 SEM image of synthesized silica particles with average size of 220 nm.

The superhydrophobic surface was fabricated by layer-by-layer deposition of Poly(DADMAC) and silica particles on linerboard substrate followed by a fluorination treatment. Figure 3.2 depicted the SEM micrograph of surface modified silica-coated linerboard surface which exhibited the surface was irregularly packed with multilayer of silica particles and only with a few interstices.

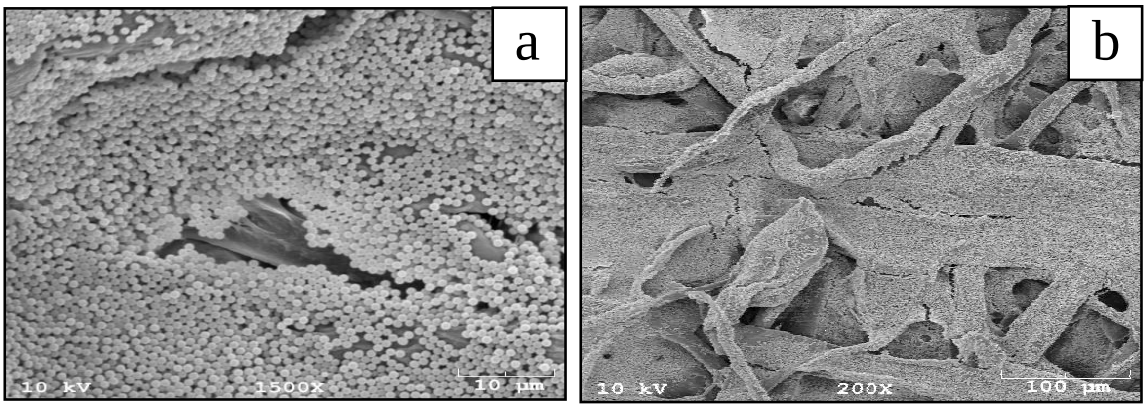

Figure 3.2 SEM images of (a) and (b) are linerboard surface coated by silica particles using layer-by-layer technique, follow by a fluorination treatment. Image of (b) is the magnification of (a).

3.1.2 Hydrophobicity of Superhydrophobic Linerboard Surface

The contact angle is the angle at which a liquid/vapor interface meets the solid surface. The contact angle is specific for any given system and is determined by the interactions across the three interfaces. Most often the concept is illustrated with a small liquid droplet resting on a horizontal solid surface. If the liquid is very strongly attracted to the solid surface the droplet will completely spread out on the solid surface and the contact angle will be close to 0°. Less strongly hydrophilic solids will have a contact angle up to 90°. If the solid surface is hydrophobic, the contact angle will be larger than 90°. On highly hydrophobic surfaces, the surfaces have water contact angles as high as 150° or even nearly 180°. On these surfaces, water droplets simply rest on the surface, without actually wetting to any significant extent. These surfaces are termed superhydrophobic. This is called the Lotus effect, as these new surfaces are based on lotus plants' surface and would be superhydrophobic. The contact angle thus directly provides information on the interaction energy between the surface and the liquid.

Because of the fast wetting of water on untreated paper surface, the water contact angles were measured right after water droplets contact sample surfaces. However, for hydrophobic linerboard specimens and superhydrophobic linerboard specimens, the contact angles were rechecked after 10 minutes of contact time. As shown in Figure 4.3, the water contact angle of linerboard surface was 51^{o}, which changed to 110^{o} on hydrophobic linerboard surface, and 155^{o} on superhydrophobic linerboard surface, indicating a superhydrophobic surface was obtained. The water contact angle results had shown, to a noticeable extent, how the surface energy and surface roughness affected the hydrophobicity of linerboard surface, and thus the water contact angle. Higher water contact angle enhanced the moisture resistance and water resistance of wood-fiber-based substrate. Furthermore, the sliding angle on such a surface was lower than 5^{o}, which meant the water droplet on the surface could roll off easily.

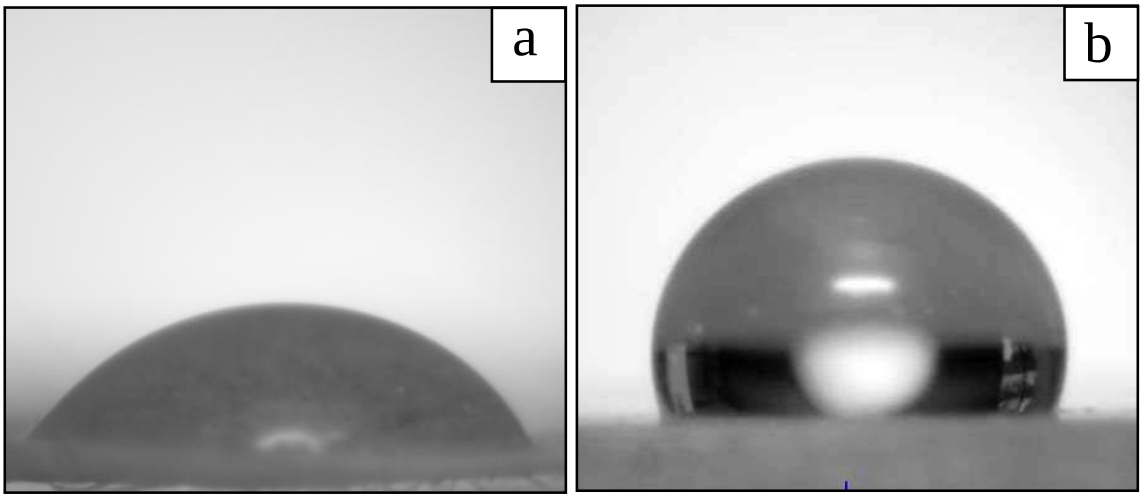

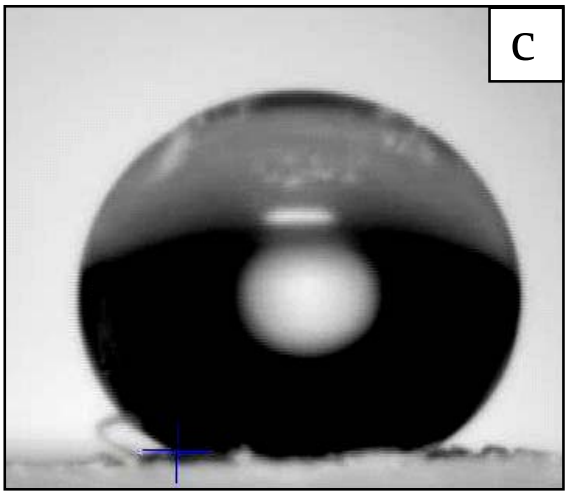

Figure 3.3 Shapes of water droplet on linerboard surface (a), hydrophobic linerboard surface (b), and superhydrophobic linerboard surface (c).

Cassie's equation, $cos\theta_A = f_1 \cos\theta - f_2$, could be used to explain the hydrophobicity of rough surface, such as treated and untreated linerboard specimens prepared in this study. Here, θ_A (110^o) was the apparent contact angle measured on the hydrophobic linerboard surface; θ (100^o) was the water contact angle on fluoridated smooth surface [38]; f_1 and f_2 were the fractions of solid surface and air in contact with water droplet, respectively, that was $f_1 + f_2 = 1$. According to the equation, the f_1 of the surface was calculated to be 0.80, which indicated that 20 % of the surface was occupied by air. However, for superhydrophobic linerboard surface, θ_A (155^o) was the apparent contact angle. According to Cassie's equation, the f_1 of superhydrophobic linerboard surface was calculated to be 0.11, which indicated that 89 % of the surface was occupied by air. The surface allowed air to be trapped more easily underneath the water droplets, so the droplets essentially rested on a layer of air. Therefore the water contact angle on the superhydrophobic linerboard surface increased significantly.

3.1.3 Surface Roughness of Superhydrophobic Linerboard Surface

Borrowing from the character of lotus leave surface, it was found that superhydrophobic property is caused by both the surface roughness and the intrinsic material hydrophobicity of the surface layer. The hydrophobic material provides the low surface energy, and the rough structure brings a large extent of air trapping when contacting with water, so the droplets essentially rested on a layer of air and can roll off easily. Rather, a significantly higher surface area compared to the projected area creates a greater energy barrier of liquid-solid interface. As shown in Section 3.1.2, the fraction of solid surface in contact with water droplet of superhydrophobic linerboard surface was calculated to be 0.11, which indicated that 89 % of the surface was occupied by air. In this section, a program is developed in MATLAB to transfer the SEM images of superhydrophobic linerboard surface to compute the fraction of solid surface in contact with water droplet of superhydrophobic linerboard surface. The developed MATLAB program is shown in Appendix A.

MATLAB is a numerical computing environment and programming language. Created by the MathWorks, MATLAB allows easy matrix manipulation, plotting of functions and data, implementation of algorithms, creation of user interfaces, and interfacing with programs in other languages. Although it specializes in numerical computing, an optional toolbox interfaces with the Maple symbolic engine, allowing it to be part of a full computer algebra system.

Figure 3.4 showed the MATLAB transferred SEM images of superhydrophobic linerboard surface with average silica particle size of 220 nm. From the transferred SEM images, around 3 layers of silica particles were packed on the linerboard surface. The

yellow circles depicted silica particles packed on the bottom layer; the pink circles depicted silica particles packed on the middle layer; and the red circles depicted silica particles packed on the top layer, which had around 9 % of projected area fraction. The result agreed with the fraction of solid surface in contact with water droplet of superhydrophobic linerboard surface which was calculated to be 0.11.

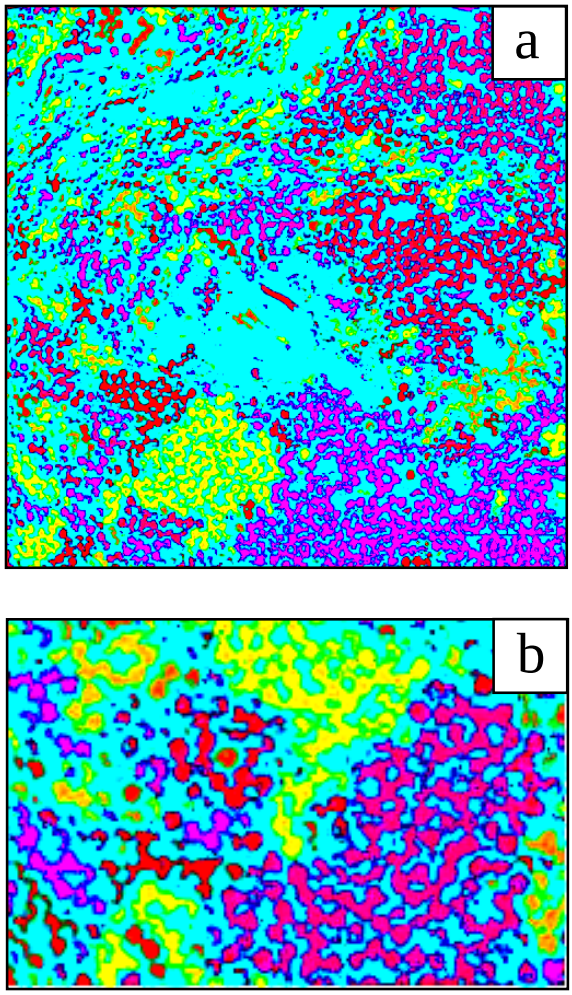

Figure 3.4 MATLAB transferred SEM images of (a) and (b) are surface modified silica-coated linerboard surface. Image of (b) is the magnification of (a).

3.1.4 Moisture Resistance of Superhydrophobic Linerboard

Properties of wood-fiber-based material were greatly dependent on its moisture content. The moisture content of specimen was measured as the ratio of the weight of water in specimen, to the weight of specimen when it was dried at 105 ^{o}C until a constant weight was obtained. In this analysis, specimens were placed in a sealed oven at ambient temperature with different relative humidity which was controlled by the amount of total water in the sealed oven for 24 hours before measuring the moisture content. Figure 3.5 showed the moisture content percentage (%) as a function of relative humidity (%) for linerboard, hydrophobic linerboard, and superhydrophobic linerboard, respectively. It was found that the moisture content of linerboard increased by about 10 % when the relative humidity increased by 70 %, which suggested the moisture absorption of linerboard increased progressively with increasing relative humidity. As compared with linerboard, the hydrophobic linerboard and superhydrophobic linerboard had much higher moisture resistance. The moisture content of hydrophobic linerboard specimens and surface superhydrophobic linerboard specimens only increased for around 1 % when the relative humidity was increased by 70 %. Nevertheless, the superhydrophobic linerboard had almost the same moisture resistance as the hydrophobic linerboard.

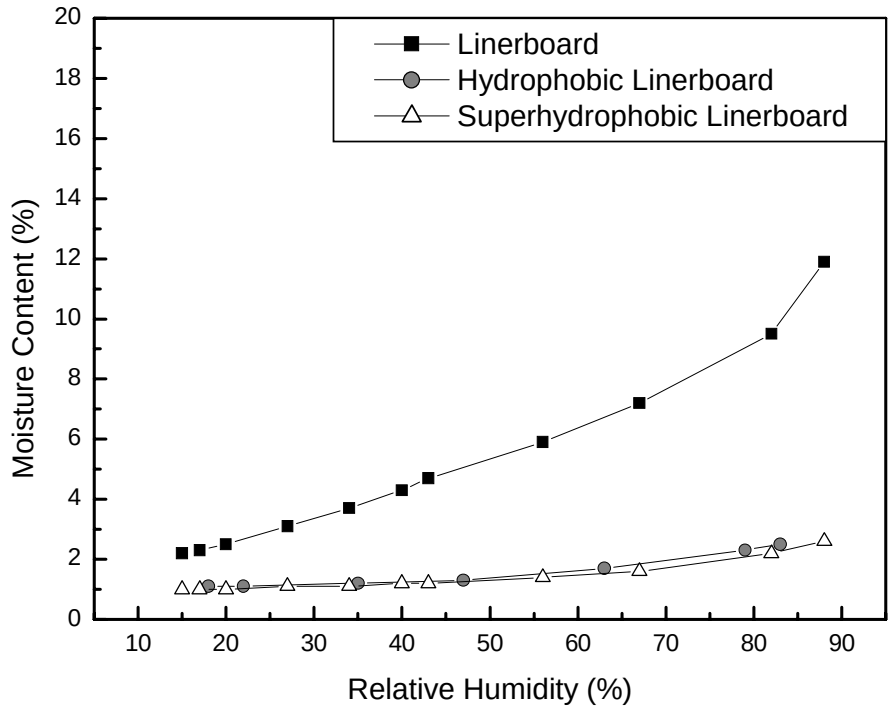

Figure 3.5 Moisture content vs. relative humidity of linerboard, hydrophobic linerboard, and superhydrophobic linerboard.

3.1.5 Tensile Strength of Superhydrophobic Linerboard

In this analysis, the tensile strength of specimen was measured after the specimens being conditioned at ambient temperature with different relative humidity that was controlled by the amount of total water in the sealed box for 12 hours. Figure 3.6 showed the tensile strength (kN/m^2) against relative humidity (%) for original linerboard, hydrophobic linerboard, and superhydrophobic linerboard, respectively. As we expected, the tensile strength of linerboard specimens decreased significantly under high relative humidity condition. As compared with linerboard, hydrophobic linerboard presented higher moisture resistance, and thus the tensile strength. The tensile strength of hydrophobic linerboard specimens decreased slightly under high relative humidity

condition. For superhydrophobic linerboard specimens, it was found that the tensile strength decreased slightly under high relative humidity condition. It was also noted that the tensile strength of the superhydrophobic linerboard was about 30% higher than hydrophobic linerboard. The reason for that might be due to the increase in the basis weight and bonding by both poly(DADMAC) and silica particles. The high strength of both hydrophobic and superhydrophobic linerboards under high humidity condition suggested that the fiber-fiber bonds were well protected in these surface modified linerboard specimens, so the moisture did not wet the linerboard specimens as it did in original linerboard specimens, as discussed in Section 3.4.

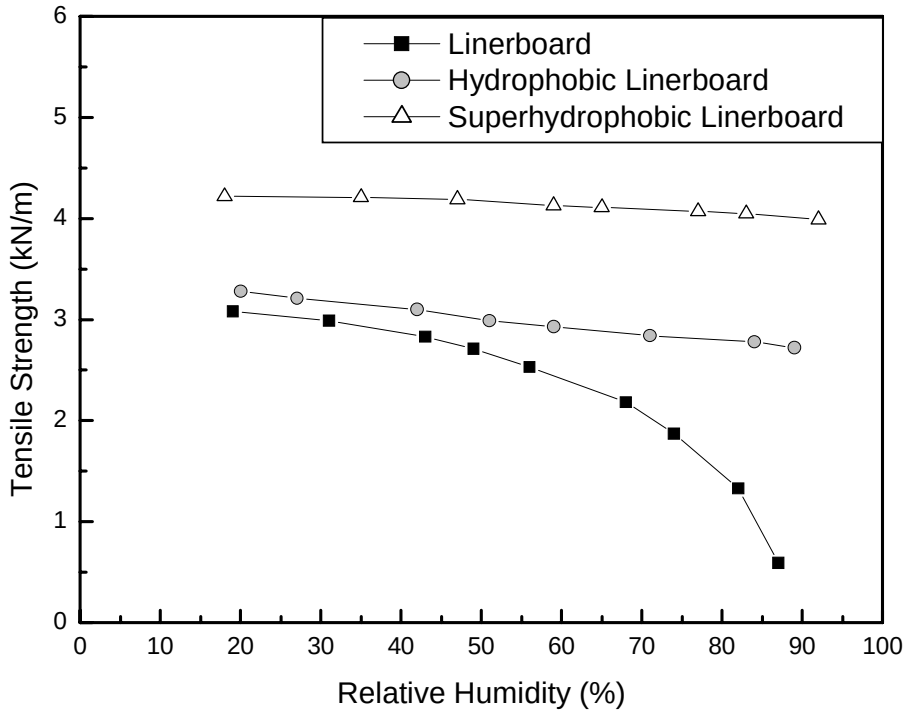

Figure 3.6 Tensile strength vs. relative humidity of linerboard, hydrophobic linerboard, and superhydrophobic linerboard.

3.1.6 Water Resistance of Superhydrophobic Linerboard

With hydroxyl groups covering the surface, wood-fiber-based materials were very hydrophilic and could absorb water or disperse in water easily. However, in the package applications, high water resistance fibers or papers were required. In this study, the water resistance of superhydrophobic linerboard was investigated. The experiments were carried out by immersing superhydrophobic linerboard specimens in water up to several hours followed with measuring the moisture content (%) and the water contact angle (degree) of the specimens. As shown in Figure 3.7, it was found that the moisture content increased to 6 % after the specimen was fully immersing in water to 1 hour. The moisture content kept around 6 % after 72 hours, and the water contact angle checked by contact angle analyzer could be kept above 150^{o} in the whole process. That demonstrated that the extremely high water resistance of superhydrophobic linerboard was developed.

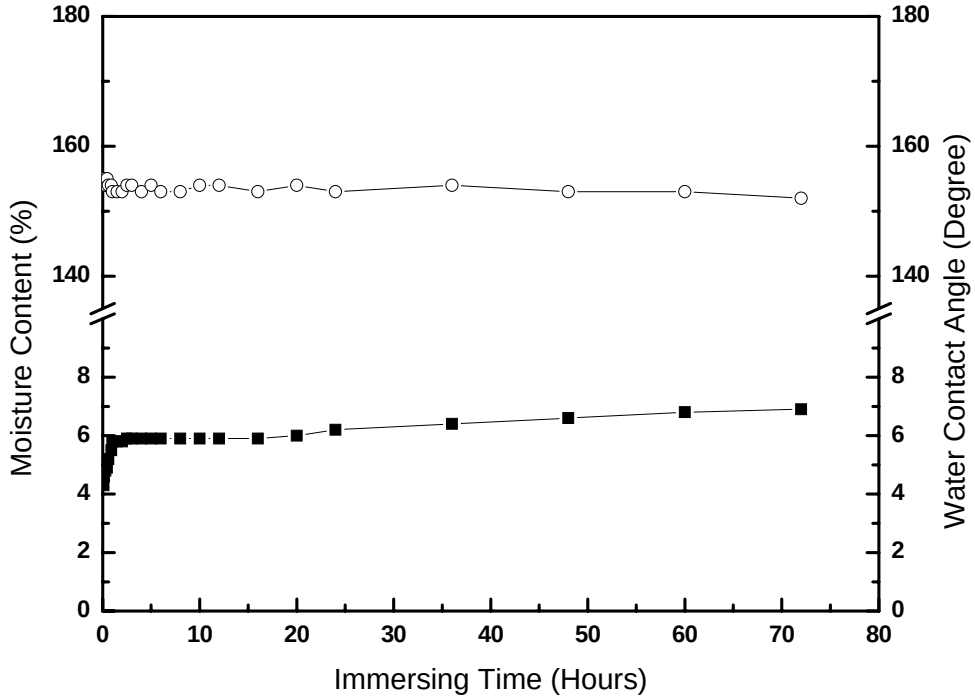

Figure 3.7 Moisture content (solid-square) and water contact angle (open-cycle) vs. immersing time of superhydrophobic linerboard.

3.1.7 Anti-contamination of Biomaterials Performance

A water droplet on an inclined superhydrophobic surface did not slide off, but it rolled off. When the water droplet rolled over a contamination, the contamination was removed from the surface if the force of absorption of the contamination was higher than the static friction force between the contamination and the surface. Usually the force needed to remove a contamination was very low due to the minimized contact area between the contamination and the superhydrophobic surface. As a result, the droplet cleaned the surface by rolling off the surface. When the bacterial water-based solution contacted the superhydrophobic linerboard surface, it was expected that the bacterial solution could be removed easily, and thus the superhydrophobic linerboard surface could prevent the contamination.

The anti-contamination of biomaterials performance of original linerboard, hydrophobic linerboard, and superhydrophobic linerboard were evaluated by measuring the contamination units of the bacteria after the paper specimens contacted with Escherichia coli-AmpicillinR solution. The flow charts were shown in Figure 3.8. During the experiment, the paper specimens with different hydrophobicities were cut into $15\times7.25\times0.4$ cm^3, and placed on a plastic film. About 0.01 ml of Escherichia coli-AmpicillinR solution with 10^5 colony forming units per milliliter (CFU/ml) was uniformly sprayed on the surface of paper specimens. In this study, the paper samples were divided in to two groups. Each group has original linerboard, hydrophobic linerboard, and superhydrophobic linerboard specimens. The first group of the specimens was offered an inclining angle of 5^o for 5 seconds right after the Escherichia coli-AmpicillinR was sprayed, and then the specimens were submerged in Luria-Bertani

(LB) medium, respectively. The second group of the specimens was submerged in water for 1 second right after the Escherichia coli-AmpicillinR was sprayed, and then the specimens were submerged in LB broth medium, respectively. The specimens were fully immersed in LB broth medium and cultured at 37^{o}C for 24 hours before measuring the equivalent colony forming units (CFU). All the experiments were performed in dark. The CFU of Escherichia coli-AmpicillinR incubated in LB broth medium presented the Escherichia coli-AmpicillinR units on the specimens before incubation.

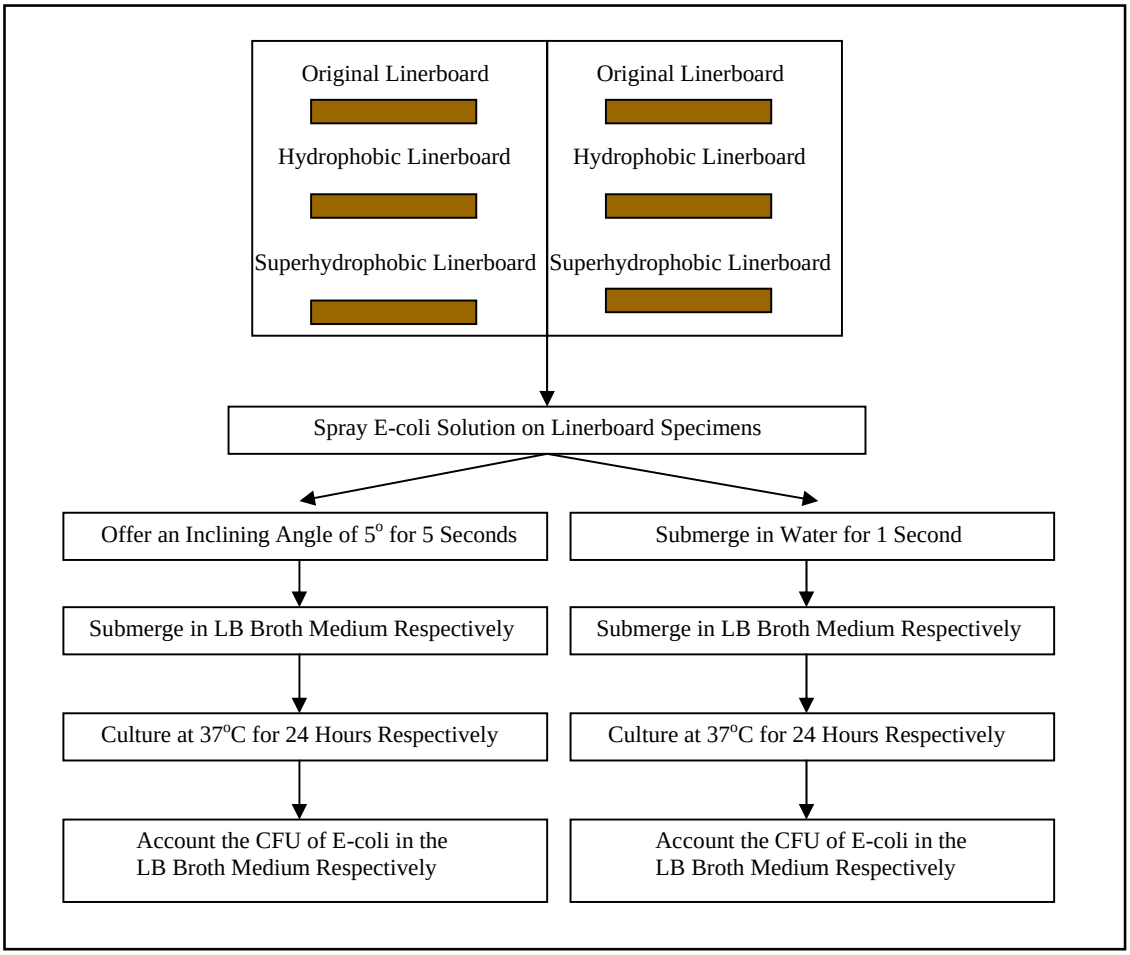

Figure 3.8 Flow charts of the anti-contamination of biomaterials performance process.

Figure 3.9 displayed the CFU of Escherichia coli-Ampicillin^{R} on original linerboard, hydrophobic linerboard, and superhydrophobic linerboard specimens for 2 groups of the samples. For the first group, it was found that the CFU of Escherichia coli-Ampicillin^{R} on the specimens decreased as the hydrophobicity of specimen increased. Compared with original linerboard specimens, approximate 70 % of bacteria were left on the hydrophobic linerboard specimens and approximate 7 % of bacteria were left on the superhydrophobic linerboard specimens. The significant lower of the bacterial contamination on the superhydrophobic linerboard specimens than hydrophobic linerboard specimens was due to the factor that the E-coli solution rolled off from the surface of superhydrophobic linerboard specimens, but adhered on the surface of hydrophobic linerboard specimens when an inclining angle of 5^{o} was applied to the specimens. For the second group, the CFU of Escherichia coli-Ampicillin^{R} on the specimens decreased intensely as the hydrophobicity of specimen increased. As compared with the original linerboard specimens, there were only about 30 % of bacteria remained on the hydrophobic linerboard specimens and less than 1 % of bacteria remained on the superhydrophobic linerboard specimens. It was noted that the bacteria on the superhydrophobic linerboard specimens was much easier to be removed by immersing contaminated paper in water. As discussed before, the water resistance increased as the hydrophobicity of the linerboard surface increased. With higher anti-wetting property, the bacteria could be washed easier. The results shown in Figure 3.9 clearly demonstrated that superhydrophobicity of a substrate plays an important role in fabricating anti-biological contamination materials.

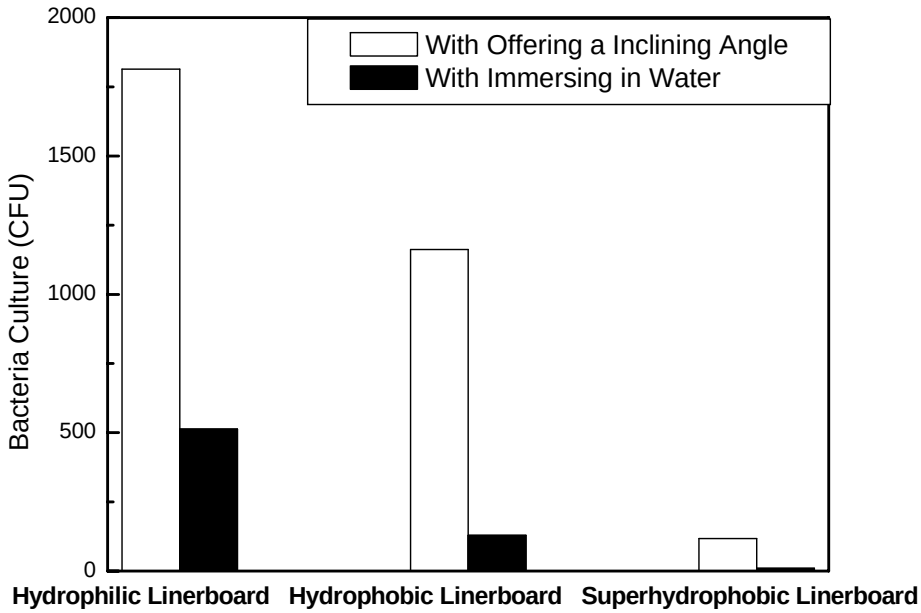

Figure 3.9 Bacteria culture on linerboard, hydrophobic linerboard, and superhydrophobic linerboard surfaces after offering an inclining angle of 5^{o} for 5 seconds (White) and with fully immersing in water for 1 second (Black).

The linerboard specimens with different hydrophobicities were prepared by layer-by-layer deposition of poly(diallyldimethylammonium chloride) (poly-DADMAC)/ different sizes of silica particles followed with a fluorination treatment. The water contact angles and the sliding angles of the linerboard specimens were measured as shown in Figure 3.10. Sliding angle was the angle when a droplet of water of a certain weight begins to slide down an inclined plate. The sliding angle was commonly employed as a criterion for assessing the hydrophobicity of a solid surface. It was found that the sliding angle decreased with the water contact angle increasing. It was also noted that the sliding angles were lower than 5^{o} as the water contact angles were larger than 150^{o}, which indicated the superhydrophobic linerboard with a impressive self-cleaning property.

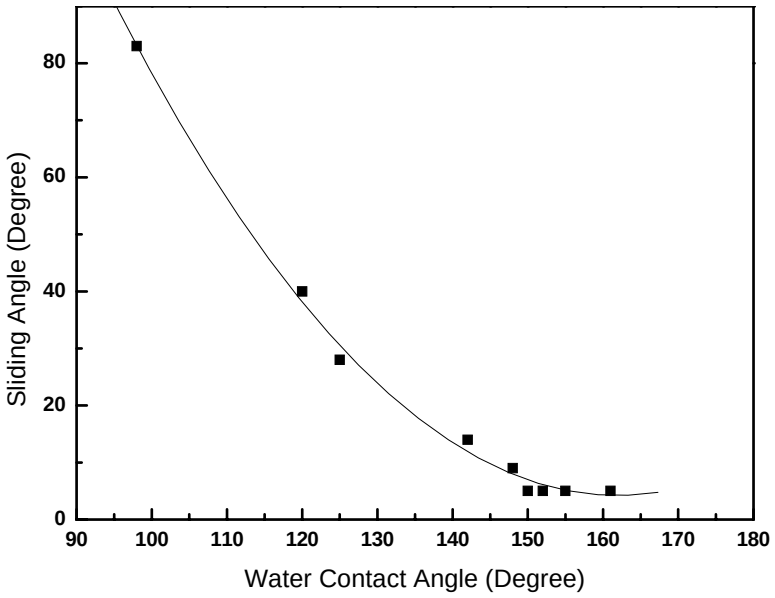

Figure 3.10 Sliding angles against water contact angles on linerboard specimens.

The sliding angle on the superhydrophobic paper was lower than 5^{o}, which meant the bacteria droplets on the superhydrophobic linerboard surface could be rolled off after the surface was offered an inclining angle of 5^{o}. However, it was found that some bacteria were remained after offering an inclining angle of 5^{o} in Figure 3.11. The major reason could be the micro-porous linerboard surface trapped some of the bacteria droplets, although the surface was superhydrophobic. To demonstrate that, inclining angle effect on superhydrophobic linerboard surface was studied. The superhydrophobic linerboard specimens were offered with different an inclining angles for 5 seconds respectively right after the Escherichia coli-Ampicillin^{R} was sprayed, and then the specimens were submerged in LB broth medium. The culturing process was the same as before. Figure 8 displayed the equivalent colony forming units (CFU) of bacteria against different inclining angles. The CFU on the superhydrophobic linerboard surface decreased significantly after the specimen was offered a small inclining angle, and the CFU

decreased gradually with the inclining angle increasing. After offering an inclining angle of 90^{o}, no bacterium was remained on the superhydrophobic surface. The results reflected the bacteria cannot contaminate the superhydrophobic surface at this condition even though the superhydrophobic paper has large porous on its surface.

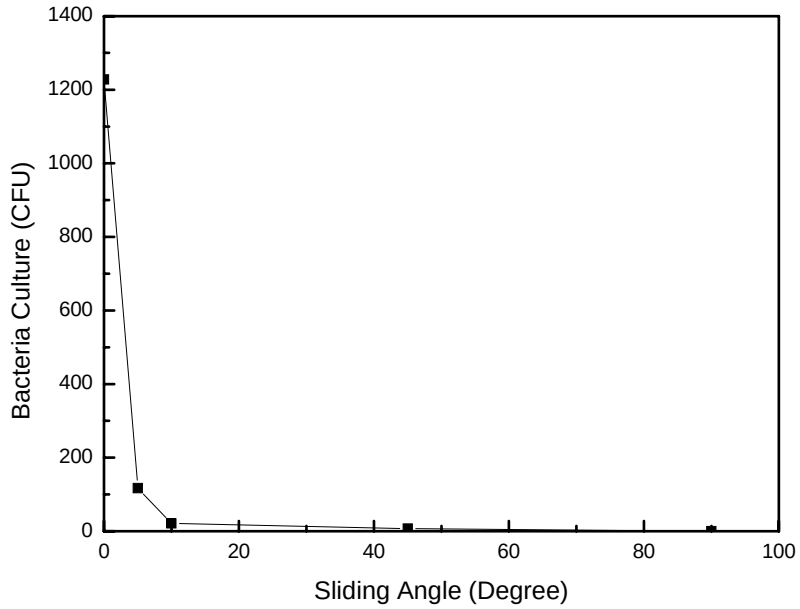

Figure 3.11 Bacteria culture on superhydrophobic linerboard surface after offering a sliding angle for 5 seconds.

3.1.8 Viscosity of Liquid Effect of Superhydrophobic Linerboard

It was well known the nanostructures and the low surface energy on superhydrophobic surface allowed air to be trapped more easily underneath water droplets, so the water droplets could be removed easily. Contrary to hydrophilic liquids, hydrophobic liquids could replace the trapped air on the superhydrophobic surface, and penetrated the substrate. It was also known viscous liquids had high resistance to flow, which caused viscous liquids difficult to replace the trapped air. Thus the contact angle against viscous liquid was high. To demonstrate that superhydrophobic surface could prevent the contaminations from viscous hydrophobic liquids, the polystyrene/THF mixtures with different viscosities were applied to the study.

In this study, contact angles of the polystyrene/THF mixtures with various weight ratios were measured on the linerboard, hydrophobic linerboard, and superhydrophobic linerboard surfaces at room temperature. Viscosities of the polystyrene/THF mixtures were measured by Cannon-Fenske Routine viscometer at room temperature. The results were shown in Figure 3.12.

It indicated that the viscosities of polystyrene/THF mixtures increased with the polystyrene/THF weight ratios. The contact angle increased with the increasing of polystyrene/THF mixture viscosity, but the contact angle was not sensitive to the viscosity of polystyrene/THF mixture. The contact angle increased with the increasing of mixture viscosity was due to the viscous liquids filled the microstructures slowly and allow air to be trapped longer. However, the contact angles of polystyrene/THF mixture on linerboard surface were under 90^{o}, which indicated the original linerboard surface could be wetted even against viscous liquids.

The contact angles of polystyrene/THF mixture on hydrophobic linerboard surface were also shown in Figure 3.12. The contact angle increased with the increase polystyrene/THF mixture viscosity, and reached 90^o where the viscosity of polystyrene/THF mixture was higher than 20 cP. It revealed the hydrophobic linerboard surface could not be wetted only against viscous liquids. Although the polystyrene/THF mixture gradually filled the microstructure on hydrophobic linerboard surface when the viscosity of mixture was low. Compared with hydrophilic linerboard, the higher hydrophobicity on hydrophobic linerboard surface enable air to be trapped on the surface when the viscosity of mixture was high.

It was found that on the superhydrophobic linerboard surface, the contact angle of the polystyrene/THF mixture increased with the increase of the polystyrene/THF mixture viscosity on superhydrophobic linerboard surface. The increase process could be divided into two stages with 1 cP of viscosity as the inflexion. In the first stage, the contact angles of the polystyrene/THF mixture with viscosities lower than 1 cP was sensitive to of viscosity. In the second stage where the viscosities were higher than 1 cP, the contact angles increased slowly from 130^o to 150^o, which indicated the contact angles of polystyrene/THF mixtures with viscosities higher than 1 cP were not sensitive.

Compared with hydrophobic linerboard, it was observed the contact angles on superhydrophobic linerboard surface increased significantly with slight increase of polystyrene/THF mixture viscosity. It revealed the structures on linerboard surface affect the wetting behaviors. With nanostructures on superhydrophobic linerboard surface, it enable higher amount of air to be trapped on the surface, which considerable contributed to the air contact fraction and thus the contact angle.

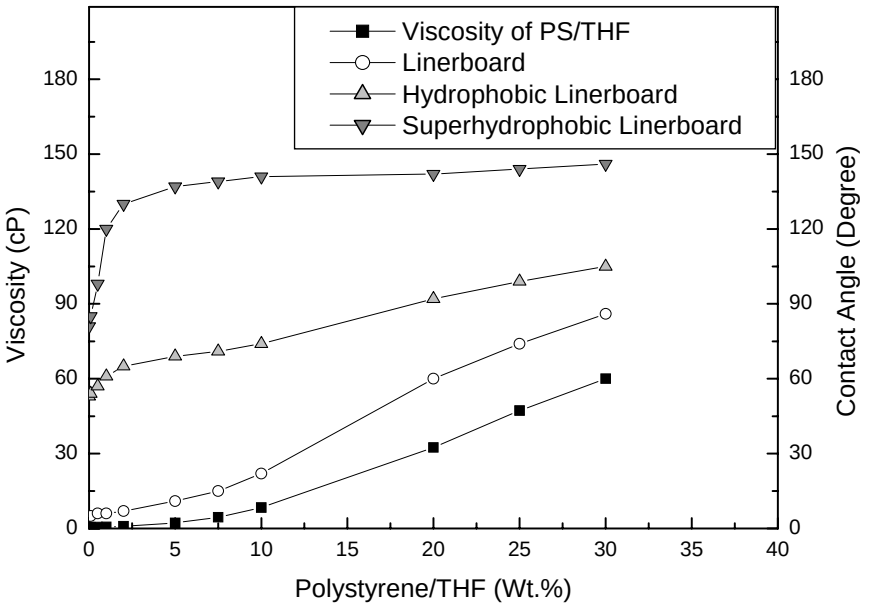

Figure 3.12 Viscosities and contact angles of polystyrene/THF mixture on the linerboard and superhydrophobic linerboard surface with different mixture weight ratios.

3.2 Particle Size Effect of Superhydrophobic Linerboard Surface

3.2.1 Surface Roughness of Superhydrophobic Linerboard Surface Coated with Different Size of Silica Particles

It was well known that the nano-scaled surface roughness is one of the critical factors for creating a superhydrophobic surface. In the study, silica spherical particles with different particle sizes were used respectively for the surface roughness treatment as shown in Figure 3.13. After fluorination treatment, the hydrophobicity of surface was then characterized by contact angle analyzer. As shown in Figure 3.14, the water contact angle changed from 110^{o} on hydrophobic linerboard specimen surface, to 155^{o}, 152^{o}, 150^{o}, and 145^{o} on the superhydrophobic linerboard specimens coated with 220 nm, 420 nm, 680 nm and 1000 nm of silica particles, respectively. It was found that the water contact angle increased significantly from hydrophobic linerboard surface to superhydrophobic linerboard surface and the water contact angle decreased slightly on superhydrophobic linerboard surface as the silica particle size increased. The results suggested that the superhydrophobic surface was successfully created by introducing the nano-scaled surface roughness.

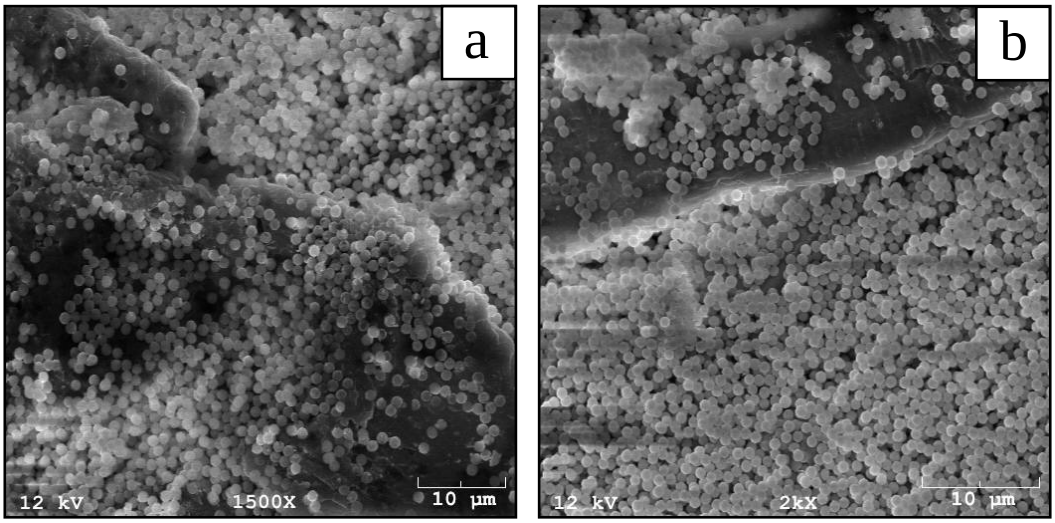

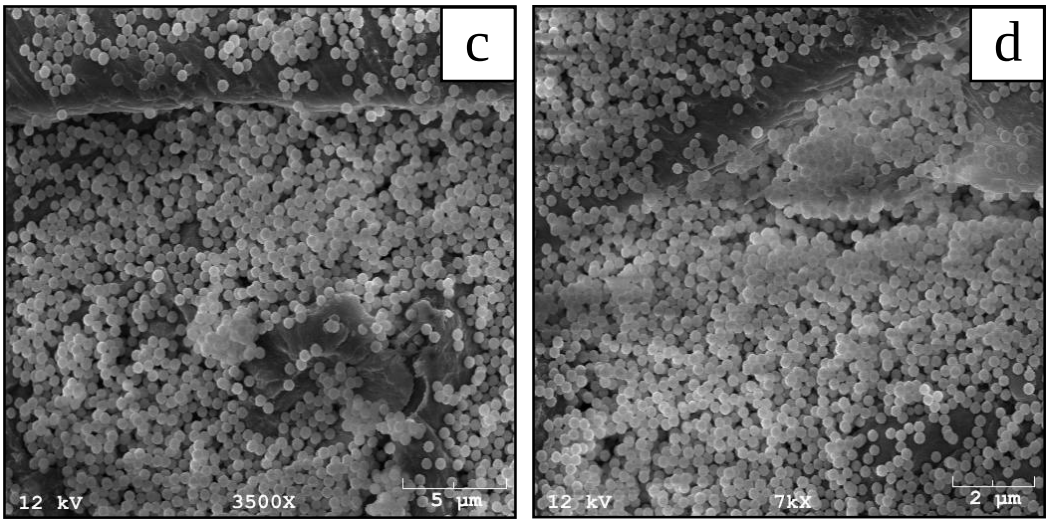

Figure 3.13 SEM images of (a) surface modified silica-coated linerboard surface with average silica particle size of 1 μm, (b) surface modified silica-coated linerboard surface with average silica particle size of 680 nm, (c) surface modified silica-coated linerboard surface with average silica particle size of 420 nm, and (d) surface modified silica-coated linerboard surface with average silica particle size of 220 nm.

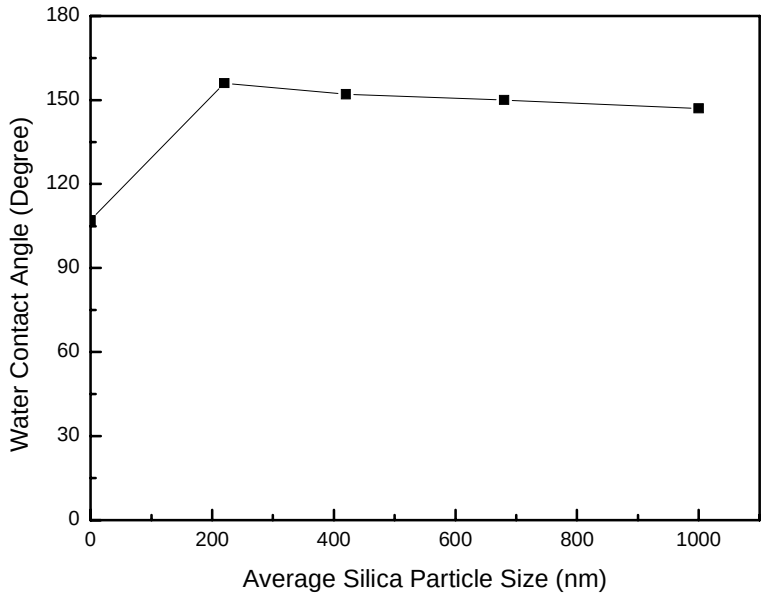

Figure 3.14 Water contact angles of surface modified silica-coated linerboard surface with different silica particle sizes.

3.2.2 Surface Roughness of Superhydrophobic Linerboard Surface Coated with Different Size Ratio of Mixed Silica Particles

Microscope observations reveal that the waxy surface of the lotus leaf is made of micron-sized bumps that, in turn, are covered with nano-scale tubes as shown in Figure 3.15. This two-fold structure traps air under any rain drops that fall on the leaf, creating a surface that efficiently repels water. In the study, the silica spherical particles with different particle size ratios were coated for the surface roughness treatment in order to increase the surface roughness. The surface roughness was increased by layer-by-layer deposition of poly(diallyldimethylammonium chloride)/ micron-scale silica particles that, in turn, were coated with nano-scale silica particles in order to bio-mimic the structure of lotus leaf surface. The surface morphologies of the silica-coated linerboard were shown in Figure 3.16. The nano-sized silica particles could not be coated evenly on the micro-sized silica particles. Rather, the nano-sized silica particle agglomerates were found in the micrographs. That was due to the nano-sized silica particles had higher surface energy comparing with micro-sized silica particles. Therefore, nano-sized silica particles aggregated and formed agglomerates.

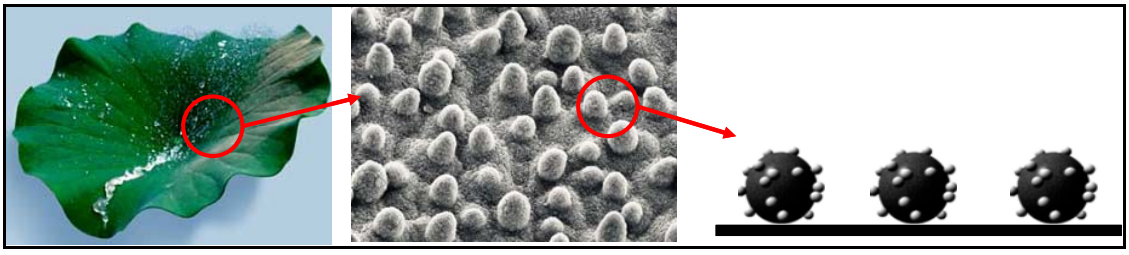

Figure 3.15 SEM image and schematic surface structure of lotus leave surface.

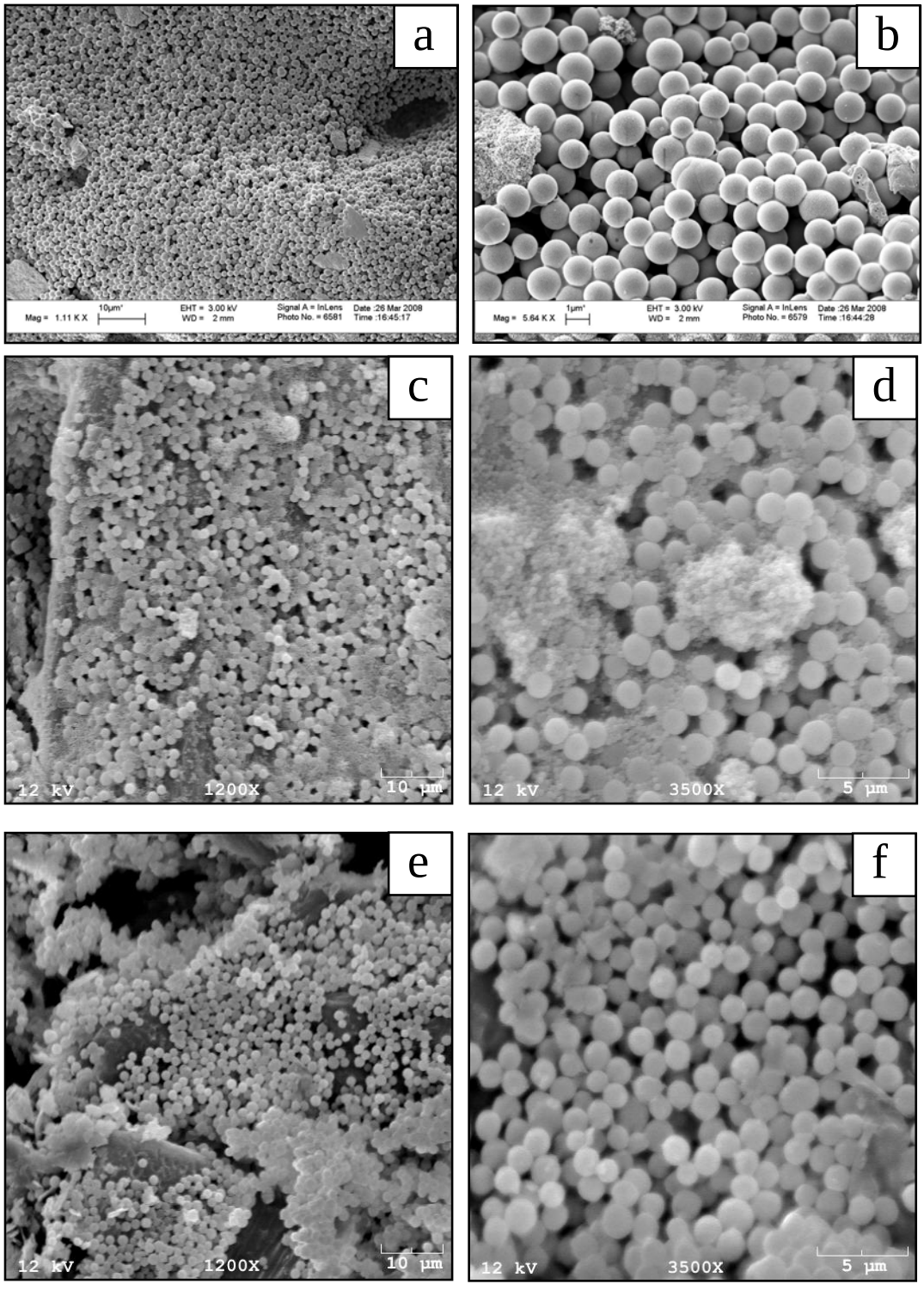
a
Mag = 1.11 K X
10µm'
EHT = 3.00 kV
WD = 2 mm
Signal A = InLens
Photo No. = 6581
Date :26 Mar 2008
Time :16:45:17
b
Mag = 5.64 K X
1µm'
EHT = 3.00 kV
WD = 2 mm
Signal A = InLens
Photo No. = 6579
Date :26 Mar 2008
Time :16:44:28
c
12 kV
1200X
10 µm
d
12 kV
3500X
5 µm
e
12 kV
1200X
10 µm
f
12 kV
3500X
5 µm

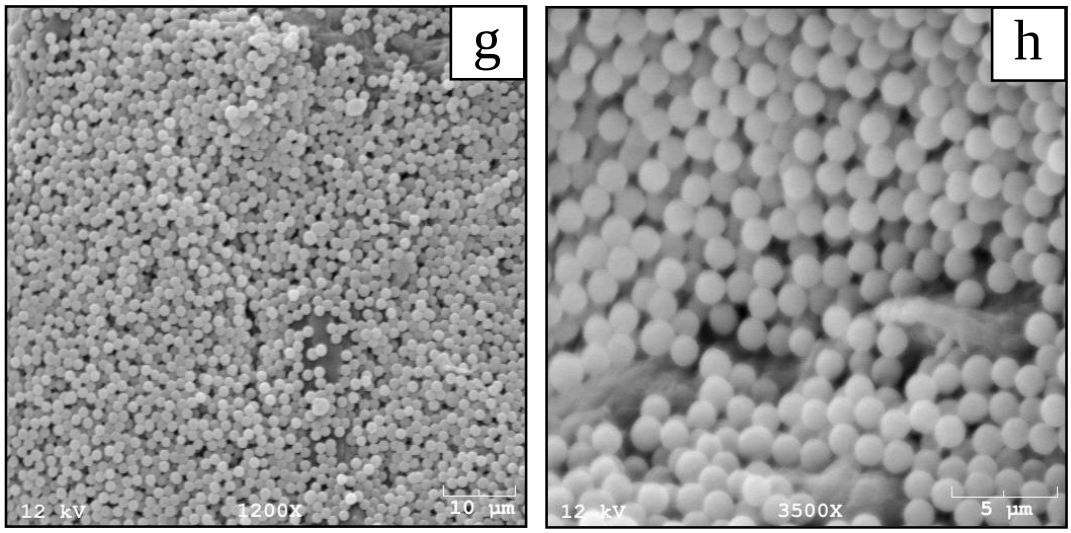

Figure 3.16 SEM images of (a) (b) surface modified silica-coated linerboard surface with average silica particle sizes of 1 μm and 75 nm, image of (b) is the magnification of (a); (c) (d) surface modified silica-coated linerboard surface with average silica particle sizes of 1 μm and 220 nm, image of (d) is the magnification of (c); (e) (f) surface modified silica-coated linerboard surface with average silica particle sizes of 1 μm and 420 nm, image of (f) is the magnification of (e); (g) (h) surface modified silica-coated linerboard surface with average silica particle sizes of 1 μm and 800 nm, image of (h) is the magnification of (g).

After fluorination treatment, the hydrophobicity of surface was then characterized by contact angle analyzer. As shown in Figure 4.17 and Figure 4.18, the water contact angle increased significantly from hydrophobic linerboard surface to superhydrophobic linerboard surface and the water contact angle decreased slightly on superhydrophobic linerboard surface as the nano-sized silica particle size increased. The results suggested that the superhydrophobic surface was successfully created by introducing the surface roughness. Compared with the linerboard coated with mono-sized silica particles, the water contact angles on the linerboard coated with the mixture of silica particles with two different sizes were slightly higher. That revealed the surface roughness was not significantly increased by coating with micron-scale silica particles followed with coating with nano-scale silica particles.

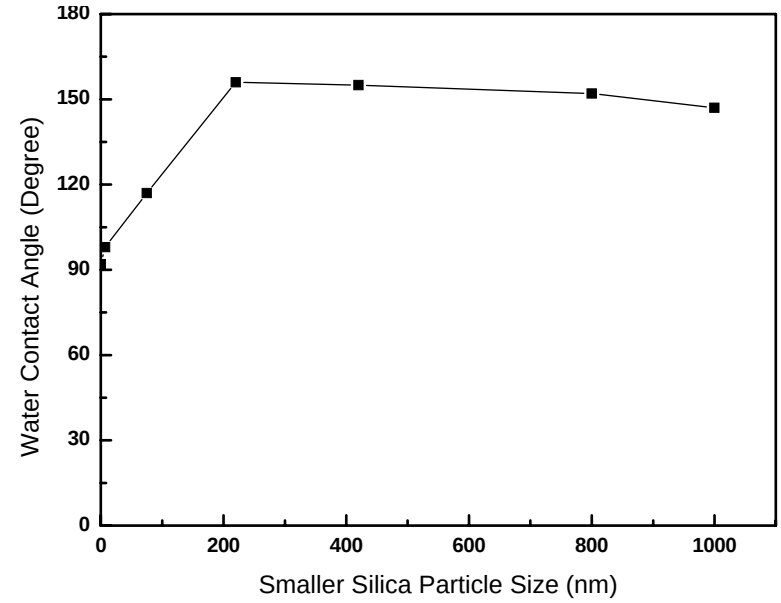

Figure 3.17 Water contact angles of surface modified silica-coated linerboard with united size of silica particles.

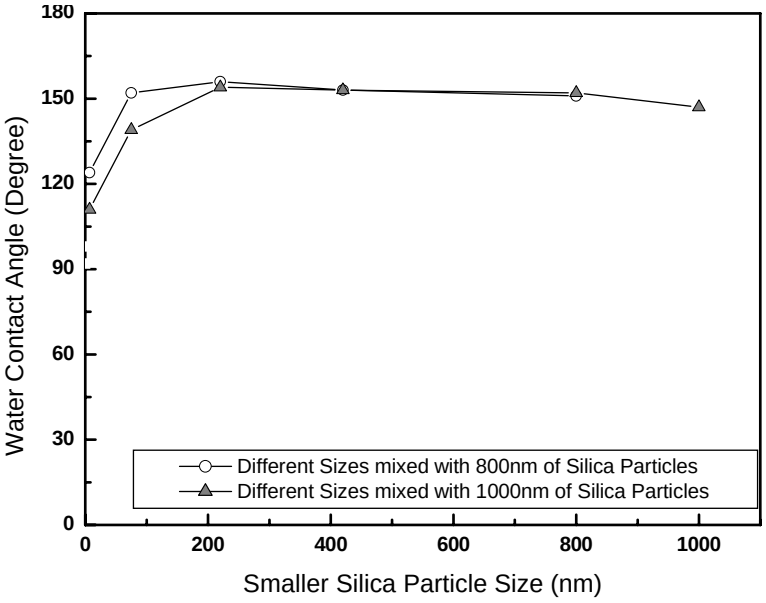

Figure 3.18 Water contact angles of surface modified silica-coated linerboard with different size ratio of silica particles.

3.3 Preparation of Superhydrophobic Linerboard with Different Methods

3.3.1 Preparation of Superhydrophobic Linerboard by Spread-coating of Silica Solution Followed by a Fluorination Treatment

Spread-coating is a simple procedure used to apply uniform thin films to substrates. However, with the negative charges on silica particle surface and wetted linerboard surface, it is difficult to spread the silica particles on the linerboard surface, and to keep the silica particles on the linerboard surface after drying. A large part of silica solution penetrated inside the micro-porous linerboard in the coating procedure. In this section, the concentration of silica solution needed to keep enough amount of silica particles on the linerboard surface was studied.

First of all, 420 nm size of silica particles were dispersed in deionized water with different weight ratios. Before usage, the silica suspension was sonicated by ultrasonicator (W-385) for 10 minutes to disperse the silica particles in the solution. 0.1 ml of silica solution was placed on 15×7.25×0.4 mm^3 size of linerboard substrate, and the coating solution was then spread on the linerboard surface. After drying, the silica-coated substrate was placed in a sealed vessel, on the bottom of which was dispensed a smaller unsealed vessel within a small amount of POTS. The sealed vessel was then put in an oven at 125 °C to enable the silane group of POTS vapor to react the hydroxide group on the silica-coated substrate surface. After 2.5 hours, the substrate was removed to another clean sealed vessel and heated at 150 °C for another 2.5 hours to volatilize the unreacted POTS molecules on the substrate. In short, the linerboard specimens with different hydrophobicities were fabricated by spread coating of difficult concentration of silica solution on linerboard substrate followed by a fluorination treatment.

The surface morphologies of the linerboard specimens were shown in Figure 3.19. The amount of silica particles kept on the linerboard surface increased as the concentration of silica solution increased. That was due to the viscosity increased with the concentration of the silica solution, and the higher solution viscosity prevented the penetration of silica solution. So, larger amount of silica particles was left on the linerboard surface, and thus caused higher roughness. Therefore the water contact angle increased with the concentration of silica solution which was shown in Figure 3.20. It showed the water contact angle reached 150^{o} as the concentration of silica solution equaled to 5 %, which indicated the superhydrophobic surface could be prepared by spread coating 5 % of silica solution on linerboard followed by a fluorination treatment.

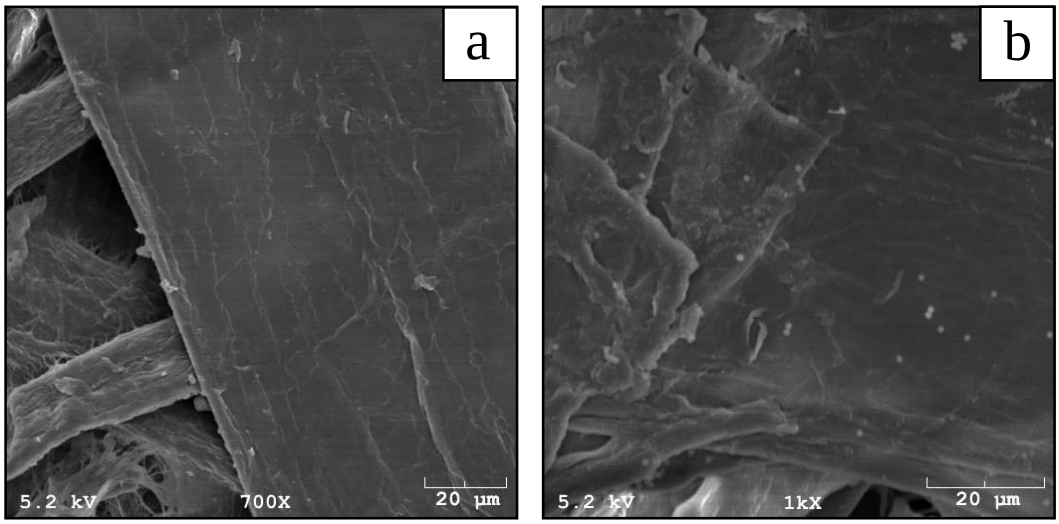

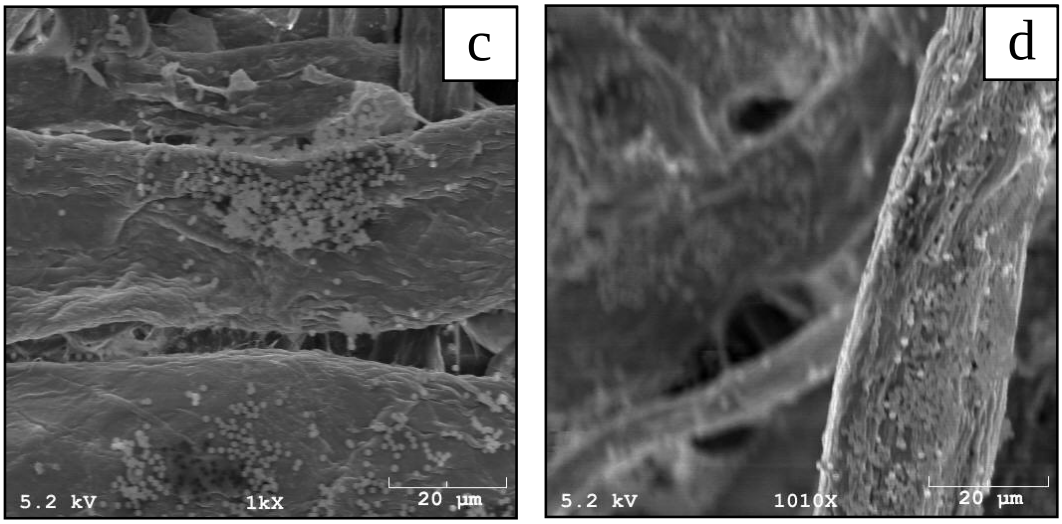

Figure 3.19 SEM images of (a) surface modified linerboard without silica particles, (b) surface modified silica-coated linerboard coated with 2 % of 420 nm silica solution, (c) surface modified silica-coated linerboard coated with 5 % of 420 nm silica solution, and (d) surface modified silica-coated linerboard coated with 10 % of 420 nm silica solution.

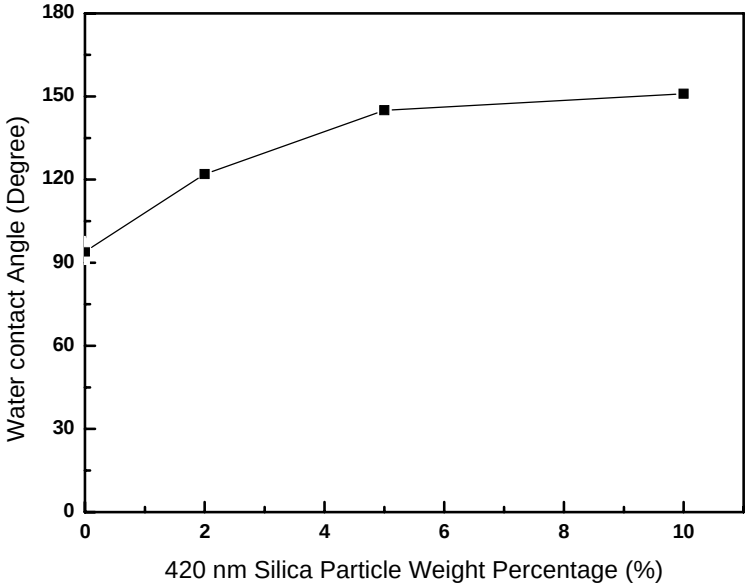

Figure 3.20 Water contact angles of surface modified silica-coated linerboard surface with different weight ratio of silica solutions.

3.3.2 Preparation of Superhydrophobic Linerboard by Dip-coating in Cationic Starch Solution and Silica Solution Followed by a Fluorination Treatment

Dip-coating refers to the immersing of a substrate into a solution of the coating material, removing the piece from the solution, and allowing it to drain. It is a popular way of creating thin film coated materials. Oji ACE-K-100 cationic starch and anionic silica particles were used in the dip coating procedure. First of all, 1.3 g of cationic starch was dispersed in 8.7 g of deionized water. Before usage, the cationic starch suspension was heated at 85 ^{o}C for 10 minutes to well disperse the cationic starch in the solution. Secondly, silica particles of 420 nm were dispersed in deionized water with different weight ratios. Before usage, the silica suspension was sonicated by ultrasonicator (W-385) for 10 minutes to disperse the silica particles in the solution. The negative charged linerboard substrate was first immersed in prepared cationic starch solution for 10 seconds to render the substrate positively charged, followed by immersing in silica solution for 10 seconds. After drying, the surface property of silica-coated substrate was modified by a fluorination treatment in the same procedure as before. In short, the linerboard specimens with different hydrophobicities were fabricated by dip-coating of difficult concentration of silica solution on linerboard substrate followed by a fluorination treatment.

The surface morphologies of the linerboard specimens were shown in Figure 3.21. The amount of silica particles on the linerboard surface increased as the concentration of silica solution increased, and the serious silica agglomeration was found on the silica-coated linerboard surfaces. From Figure 3.22, the water contact angles reached 140^{o} on the surface modified silica-coated linerboard coated with 1 % of silica solution, and kept

around 140^{o} on the surface modified silica-coated linerboard surface coated with higher concentration of silica solution. Compared with layer-by-layer deposition method and spread-coating method, a large amount of silica particles was easier to keep on the surface in the dip-coating procedure, and the procedure was simpler. However, we had not been able to uniformly coat silica particles on the linerboard. The SEM micrographs indicated that only part of the linerboard was coated alone with cationic starch, so the surface roughness was not high enough to prepare superhydrophobic surface.

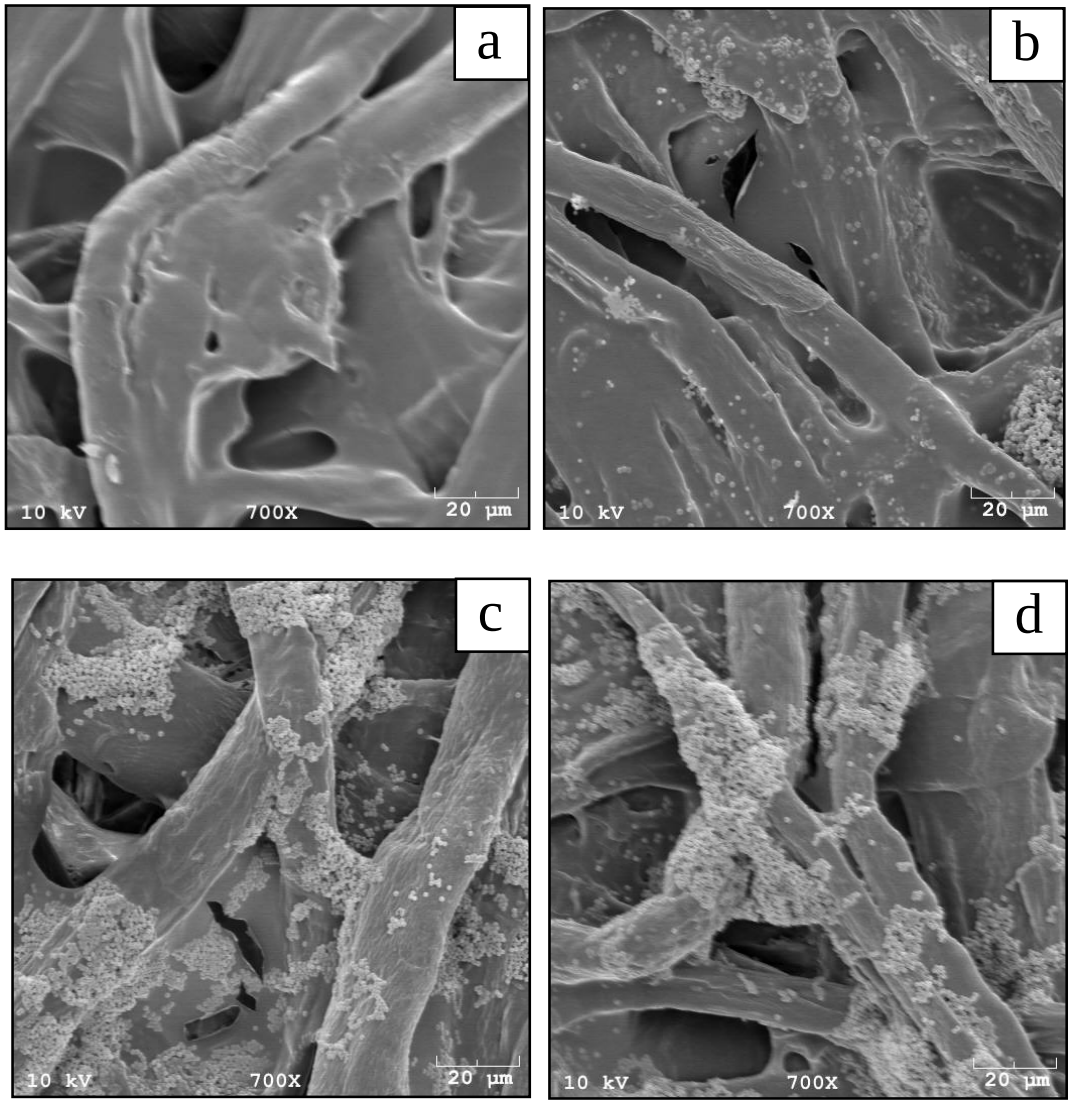

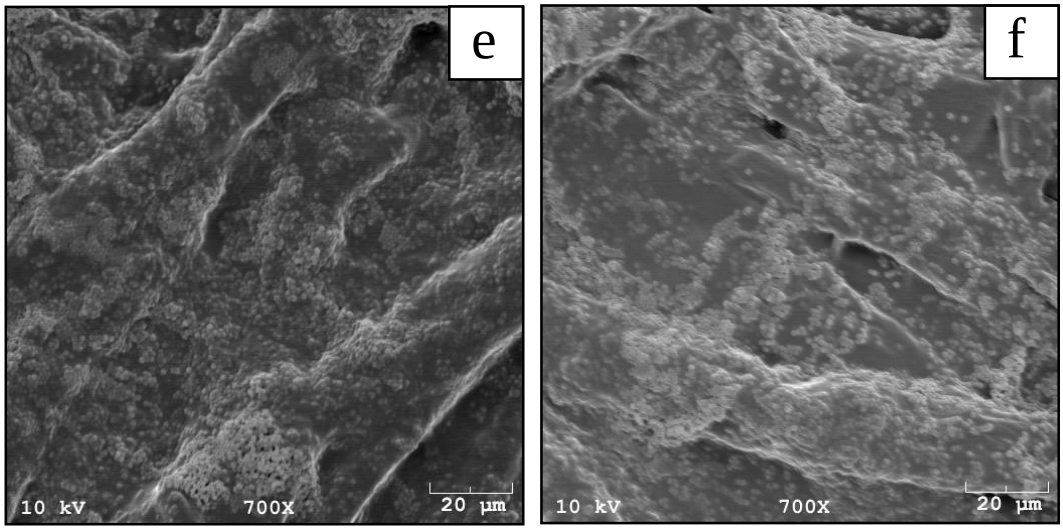

Figure 3.21 SEM images of (a) surface modified linerboard with cationic starch only, (b) surface modified silica-coated linerboard coated with 0.5 % of 420 nm silica solution, (c) surface modified silica-coated linerboard coated with 1 % of 420 nm silica solution, (d) surface modified silica-coated linerboard coated with 2 % of 420 nm silica solution, (e) surface modified silica-coated linerboard coated with 5 % of 420 nm silica solution, and (f) surface modified silica-coated linerboard coated with 10 % of 420 nm silica solution.

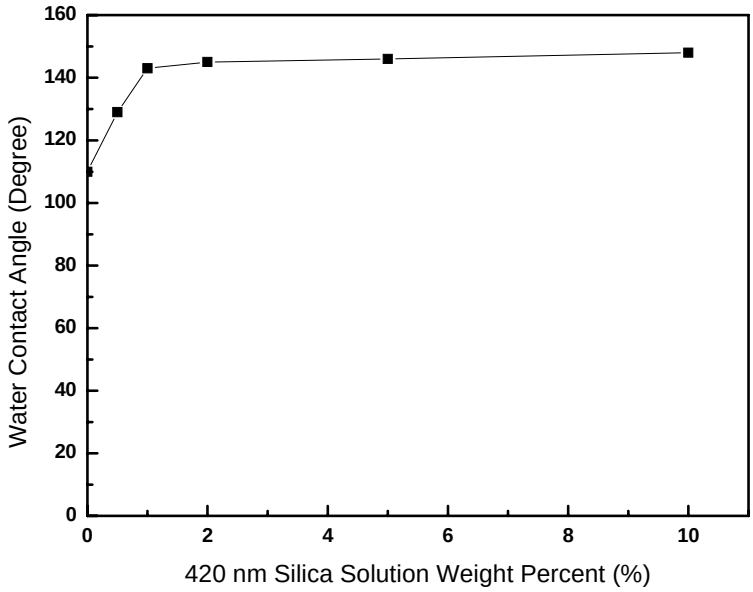

Figure 3.22 Water contact angles of surface modified silica-coated linerboard with different weight ratio of silica solutions.

3.3.3 Preparation of Superhydrophobic Linerboard by Directly Synthesizing Silica Particles on Surface Followed by a Fluorination Treatment

With anionic charges on silica particle surface and wood-fiber based substrate, it is difficult to coat the silica particles evenly and keep the particles on the linerboard surface. In the study, silica particles were chemically bonded to the linerboard to keep the surface roughness. After immersing linerboard specimens in a mixture of TEOS and ethanol, NH_4OH was added in the solution as a catalyst. According to the process described by Stober et al., TEOS was hydrolyzed to form silica particles in ethanol with a catalyst, NH_4OH, at room temperature over a period of two days. Silica particles synthesized by the above method are hydrophilic, with hydroxide groups on the silica particle surface. With hydroxide groups on the linerboard surface, silica particles could be bonded to the linerboard surface with the presence of NH_4OH.

As shown in Figure 3.23, spherical silica particles with a narrow size distribution and smooth surface were coated on the linerboard surface. Though slight agglomeration was observed in the micrograph, the silica particles were coated on the linerboard evenly. After a fluorination treatment, the silica-coated linerboard surface with a water contact angle large than 150^o was obtained as shown in Figure 3.24, which indicated a superhydrophobic linerboard was prepared successfully in the process. However, the procedure took two days for preparing the superhydrophobic linerboard would increase the cost and limit the applications.

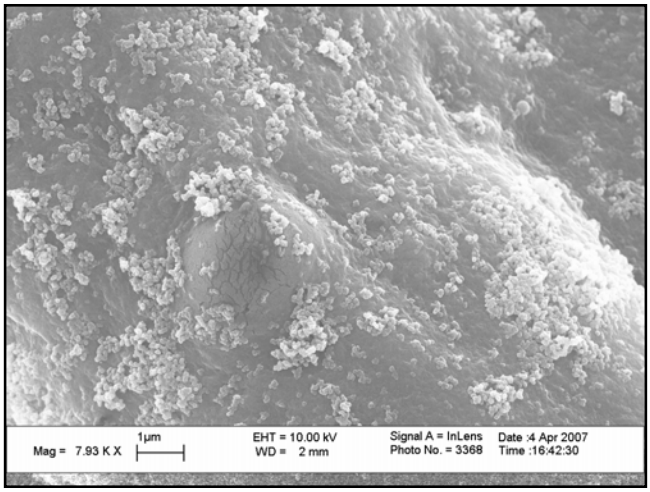

Figure 3.23 SEM images of surface modified silica-coated linerboard surface with silica particles bonding to the surface.

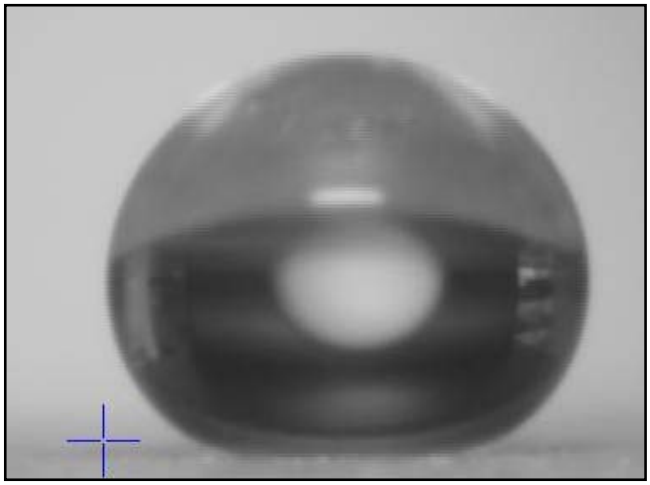

Figure 3.24 Shape of water droplet on surface modified silica-coated linerboard surface with silica particles bonding to the surface.

CHAPTER 4

CONCLUSIONS

In this work, we demonstrated that the superhydrophobic linerboard could be made by layer-by-layer deposition of poly(diallyldimethylammonium chloride)/ silica particles followed with a fluorination treatment. The fluorination treatment was carried out by chemical vapor deposition of 1H, 1H, 2H, 2H-perfluorooctyltriethoxysilane. Compared with original linerboard and chemical modified linerboard, the experiments showed that the moisture resistance, tensile strength under high relative humidity condition, water resistance, and the ability to prevent contamination of biomaterials were significantly improved by the introduction of the roughness on the surface in the combination of the decrease of the surface energy.

From the study of wetting behaviors of liquids with different viscosities, it was found the nanostructures and the low surface energy on superhydrophobic linerboard surface allowed air to be trapped more easily underneath the liquid droplets, so the droplets essentially rested on a layer of air. Rather, a significantly higher surface area compared to the projected area creates a greater energy barrier of liquid-solid interface. Coupled to this, the superhydrophobic linerboard surface enabled to repel liquid even with low viscosity that comes into contact with it.

Systematic study on the effect of surface roughness by depositing of different sized of silica particles followed with a fluorination treatment showed changes in the surface morphology and the hydrophobicity. In general, deposition of smaller particles on linerboard surface caused rougher surface, it also resulted in higher water contact

angle against the surface. The observation suggested that the increasing of surface roughness could improve the hydrophobicity of linerboard surface.

The surface roughness was increased by coating silica particles on the linerboard surface. Four different methods were introduced in the study: spread-coating of silica solution on linerboard surface; linerboard was dip-coated in cationic starch solution and silica solution; directly synthesizing silica particles on linerboard surface; and layer-by-layer deposition of poly(diallyldimethylammonium chloride)/ silica particles on linerboard surface. With negative charges on silica particle surface and linerboard surface, silica particles can not be easily coated on the linerboard surface. Compared with other methods, higher concentration of silica solution needed to be applied by using spread-coating method. In the dip-coated method, cationic starch was applied to render the surface positive charges. The silica particles could not be coated on the linerboard surface evenly. Part of the linerboard was coated alone with cationic starch, so the surface roughness was not high enough to prepare superhydrophobic surface. For directly synthesizing silica particles on linerboard surface, the procedure took much longer for preparing the superhydrophobic linerboard would increase the cost and limit the applications. Compared with the above three methods, layer-by-layer deposition method had the advantages of simplicity and low cost in fabrication, easy availability of wood-fiber-based materials, and applicability to prepare large surface area.

CHAPTER 5

FUTURE WORKS

This study focused on developing a simple and inexpensive way to prepare superhydrophobic cellulose fibers and paper products by layer-by-layer deposition of poly(diallyldimethylammonium chloride)/ silica particles on linerboard surface followed with a fluorination treatment.

Compared with other recent researches in preparing surface roughness, layer-by-layer deposition method had the advantages of simplicity and low cost in fabrication, easy availability of wood-fiber-based materials, and applicability to prepare large surface area. In this study, silica particles were synthesized and were coated on the linerboard surface to increase surface roughness. However, the silica particle synthesis procedure took several days and high cost. Therefore, using other inexpensive inorganic particles, such as nano-clay and precipitated calcium carbonate (PCC), to substitute silica particles would be an important task in the future.

In this study, 1H, 1H, 2H, 2H-perfluorooctyltriethoxysilane was applied to modify the linerboard surface by chemical vapor deposition method. Although the surface energy of fluoride was very low, and offered a great energy barrier of liquid-solid interface to repel any water that comes into contact with it. The cost of chemicals was pretty high. Compared with fluoride, alkenylsuccinic anhydride (ASA) and alkylketene dimes (AKD) were two common internal sizing agents used to resist the penetration or spreading of liquids through or on paper in the paper industry. Though the cost of the

sizing agents was lower, the surface energy of the sizing agents was not as low as fluoride. Using ASA or AKD to substitute POTS would be a challenge in the future.

Traditionally, wax and hydrophobic polymers were used to produce high water resistance packages for food and medical applications, the thick coating layer (30 to 50 μm) results in high coating cost and poor recyclability. Furthermore, the water-repellent and decomposable products obtained by regular wax or polymer coating can not greatly benefit customers and industries. Compared with wax or polymer coated paper products, less polymer was applied on the superhydrophobic paper products prepared in this research, which revealed the prepared superhydrophobic paper products were potentially repulpable. The repulping capability of this paper products could be measured to demonstrate the recycling capability.

In the study, superhydrophobic cellulose fibers and paper products were successfully prepared by layer-by-layer deposition of poly(diallyldimethylammonium chloride)/ silica particles on linerboard surface followed with a fluorination treatment. The silica particles were coated on linerboard surface by electrostatic force. Although the silica particles could be kept on the linerboard surface after immersing in water for more than three days, the silica particles could not be able to remain after applying a acute stir. The bonding strength between silica particles and cellulose fibers should be improved to augment the application areas.

APPENDIX A

MATLAB PROGRAMS

MATLAB is a numerical computing environment and programming language, which was created by the MathWorks. The MATLAB program used to transfer surface morphology images to topography images was following.

```
function [layerNum] = paper (filename)
I = rgb2gray (imread (filename));
background = imopen (I, strel('disk', 5));
I2 = imsubtract (I, background);
I3 = imadjust (I2);
level = graythresh (I3);
bw = im2bw (I3, level);
[labeled, numObjects] = bwlabel (bw, 4);
pseudo_color = label2rgb (labeled, @spring, 'c', 'shuffle');
imshow (pseudo_color);
graindata = regionprops (labeled, 'basic');
% display (max ([graindata.Area]));
% display (find ([graindata.Area] == 17709));
hist([graindata.Area], 20).
```

REFERENCES

[1] Carlson, A.B., U.S. Patent 3017373, (1962).

[2] Hart, R.T., U.S. Patent 3078181, (1963).

[3] Roberts, A., U.S. Patent 3149184, (1964).

[4] Huang, D.K., U.S. Patent 3535202, (1969).

[5] Nakashio, S., Sekine, N., Toyota, N., Fujita, F., and Domoto, M., U.S. Patent 3932912, (1976).

[6] Kelly, G.B. and Lowery, R.H.,U.S. Patent 3869296, (1975).

[7] Bateman, M.E. and Holda, E.M., U.S. Patent 3931422, (1976).

[8] Ashikaga, T. and Higashimori, S.,U.S. Patent 3679544, (1972).

[9] Hattori, T.,U.S. Patent 3740253, (1973).

[10] Gallino, R., U.S. Patent 3793067, (1974).

[11] Braidich, E.V., Gmitter, G.T., and Essen, W.J., U.S. Patent 3873480, (1975).

[12] Macleod, A.C., U.S. Patent 3875101, (1975).

[13] Chich, O.N. and Means, G.N., U.S. Patent 3849183, (1974).

[14] Downer, J.M., Hobbs, D.G., and Wootton, D.B., U.S. Patent 3859596, (1974).

[15] Mueller, G.H., and Wendel, K., U.S. Patent 3847856, (1974).

[16] Guastella, S.L., and Larrivee, J.J. U.S. Patent 3911191, (1975).

[17] Hammer, I.P., and Jakaitis, E.A., U.S. Patent 3280064, (1966).

[18] Brunsen, M.O., and McGillen, W.D., U.S. Patent 3201498, (1965).

[19] Demol, P., and Mathis, P., U.S. Patent 4476587, (1984).

[20] Hintz, H.L., and Webb, J.T., U.S. Patent 4899224, (1989).

[21] Hagenmaier, R.D. and Baker, R.A., J. Agric. Food Chem. 45, 349 (1997).

[22] Bosquez-Molina, E., Guerrero-Legarreta, I., and Vernon-Carter, E.J., Food Res. Int. 36, 885 (2003).

[23] Erlat, A.G., Henry, B.M., Ingram, J.J., Mountain, D.B., McGuigan, A., Howson, R.P., Grovenor, C.R.M., Briggs, G.A.D., and Tsukahara, Y., Thin Solid Films 388, 78 (2001).

[24] Garcia-Ayuso, G., Salvarezza, R., Martinez-Duart, J.M., Sanchez, O., and Vazquez, L., Adv. Mater. 9, 654 (1997).

[25] Ellsworth, M.W. and Novak, B.M., Chem. Mater. 5, 839 (1993).

[26] Novak, B.M., Adv. Mater. 5, 422 (1993).

[27] Schwarz, P. and Mahlke, M., Conference proceedings of 2003 TAPPI Eur. PLACE Conf. 2, 1451 (2003).

[28] Krook, M., Gallstedt, M., and Hedenqvist M.S., Packag. Technol. Sci. 18, 11 (2005).

[29] Oner, D. and McCarthy, T.J., Langmuir 16, 7777 (2000).

[30] Furstner, R., Barthlott, W., Neinhuius, C., and Walzel, P., Langmuir 21, 956 (2005).

[31] Baldacchini, T., Carey, J.E., Zhou, M., and Mazur, E., Langmuir 22, 4917 (2006).

[32] Jin, M.H., Feng, X.J., Xi, J.M., Zhai, J., Cho, K., Feng, L., and Jiang, L., Macromol. Rapid Commun. 26, 1805 (2005).

[33] Tsujii, K., Yamamoto, T., Onda, T., and Shibuchi, S., Angew. Chem., Int. Ed. 36, 1011 (1997)

.

[34] Li, H., Wang, X., Song, Y., Liu, Y., Li, Q., Jiang, L., and Zhu, D.B., Angew. Chem., Int. Ed. 40, 1743 (2001).

[35] Huang, L., Lau, S.P., Yang, H., Leong, E.S., and Yu, S.F., J. Phys. Chem. B 109, 7746 (2005).

[36] Jin, M.H., Feng, X.J., Feng, L., Sun, T.L., Zhai, J., Li, T.J., and Jiang, L., Adv. Mater. 17, 1997 (2005).

[37] Feng, L., Li, S., Li, H., Zhai, J., Song, Y., Jiang, L., and Zhu, D., Angew. Chem., Int. Ed. 41, 1221 (2002).

[38] Ebril, H.Y., Demirel, A.L., Avci, Y., and Mert, O., Science 299, 1377 (2003).

[39] Shirtcliffe, N.J., McHale, G., and Newton, M.I., Perry, C.C., Roach, P., Chem. Commun. 32, 3135 (2005).

[40] Tadanaga, K., Morinaga, J., Matsuda, A., and Minami, T., Chem. Mater. 12, 590 (2000).

[41] Nakajima, A., Abe, K., Hashimoto, K., and Watanabe, T., Thin Solid Films 376, 140 (2000).

[42] Zhao, N., Xu, J., Xie, Q.D., Weng, L.H., Guo, X.L., Zhang, X.L., and Shi, L.H., Macromol. Rapid Commun. 26, 1075 (2005).

[43] Zhang, G., Wang, D., Gu, Z.Z., and Mohwald, H., Langmuir 21, 1075 (2005).

[44] Tsoi, S., Fok, E., Sit, J.C., and Veinot, J.G.C., Langmuir 20, 10771 (2004).

[45] Sun, M.H., Luo, C.X., Xu, L.P., Ji, H., Ouyang, Q., Yu, D.P., and Chen, Y., Langmuir 21, 8978 (2005).

[46] Tavana, H., Amirfazli, A., and Neumann, A.W., Langmuir 22, 5556 (2006).

[47] Guo, Z. G., Zhou, F., Hao, J.C., and Liu, W.M., J. Am. Chem. Soc. 127, 15670 (2005).

[48] Ming, W., Wu, D., van Benthem, R., and de With, G., Nano Letter 5, 2298 (2005).

[49] Decher, G., and Hong, J.D., Makromol. Chem. Macromol Symp. 46, 321 (1991).

[50] Decher, G., Science 277, 1232 (1997).

[51] Zhang, X., and Shen, J.C., Adv. Mater. 11, 1139 (1999).

[52] Hammond, P.T., Adv. Mater. 16, 1271 (2004).

[53] Bertrand, P., Jonas, A., Laschewshy, A., and Legras, R., Macromol Rapid Commun 21, 319 (2000).

[54] Soeno, T., Inokuchi, K., and Shiratori, S., Trans. Mater. Res. Soc. Jpn. 28, 1207 (2003).

[55] Zhao, N., Shi, F., Wang, Z., and Zhang, X., Langmuir 21, 4713 (2005).

[56] Zhai, L., Cebeci, F., Cohen, R.E., and Rubner, M.F., Nano Lett. 4, 1349 (2004).

[57] Han, T.J., Zheng, Y., Cho, J.H., Xu, X., and Cho, K.O. Phys. Chem. B 109, 20773 (2005).

[58] Jisr, R.M., Ramlie, H.H., and Schlenoff, J.B., Angew. Chem., Int. Ed. 44, 782 (2005).

[59] Ji, J., Fu, J., and Shen, J.C., Adv. Mater. 18, 1441 (2006).

[60] Caruso, F., Caruso, R.A., and Mohwald, H., Science 282, 1111 (1998).

[61] Donath, E., Sukhorukov, G.B., Caruso, F., Davis, S.A., and Mohwald, H., Angew. Chem., Int. Ed. 37, 2202 (1998).

[62] Kong, W., Zhang, X., Gao, M.L., Zhou, H., Li, W., and Shen, J.C. Macromol. Rapid Commun. 15, 405 (1994).

[63] Neumann, A.W., Spelt, J.K., Applied Surface Thermodynamics 17, 2323 (1996).

[64] Wenzel, R.N., J. Phys. Colloid Chem. 53, 1466 (1949)

[65] Cassie, A.B.D., Discuss. Faraday Soc. 3, 11 (1948).

[66] Bico, J., Marzolin, C., Quéré, D., Europhys. Lett. 47, 220 (1999).

[67] Quéré, D., Physica.A 313, 32 (2002).

[68] Lafuma, A., Quéré, D., Nat. Mater. 2, 457 (2003).

[69] Stober, W., Fink, A., and Bohn, E., J. Colloid Interface Sci. 26, 62 (1968).